SHEAR AND ANCHORAGE STUDY OF REINFORCEMENT IN INVERTED T-BEAM BENT CAP GIRDERS

by

Richard W. Furlong
Phil M. Ferguson
John S. Ma

RESEARCH REPORT NO. 113-4

Research Project Number 3-5-68-113
Splices and Anchorage of Reinforcing Bars

Conducted for

The Texas Highway Department

In Cooperation with the
U. S. Department of Transportation
Federal Highway Administration

by

CENTER FOR HIGHWAY RESEARCH
THE UNIVERSITY OF TEXAS AT AUSTIN

July 1971

The opinions, findings, and conclusions expressed in this publication are those of the authors and not necessarily those of the Federal Highway Administration.

P R E F A C E

This Research Report 113-4 is the report on those phases of the general project "Splices and Anchorage of Reinforcing Bars," which relate to tests of inverted T-shaped reinforced concrete beams. It follows Research Report 113-3 "Tensile Bar Splicing" and reports studies of reinforcement for bracket design and for the design of web reinforcement in inverted T-beams. The anchorage of reinforcement used as flexural steel in brackets and reinforcement used in the web of beams received special attention in this study. Recommendations for the design of both w e b and bracket reinforcement in inverted T-beams are made as conclusions to this report.

Research Report 113-3, Part 2, included conclusions and recommendations regarding splice tests with #11, #14, and #18 reinforcing bars. It superseded previous Research Report 113-2, Part 1, on Tensile Lap Splices.

Research Report 113-1, entitled "Test of Upper Anchorage #14S Column Bars in Pylon Design," by K. S. Rajagopalan and Phil M. Ferguson, published August 1968, covers another separate phase of the project completed earlier. A later report will cover a study regarding the influences of bond creep on deflection.

Support has been provided by the Texas Highway Department and the Federal Highway Administration, U. S. Department of Transportation. The encouragement and assistance of their contact representatives are acknowledged with thanks.

Richard W. Furlong
Phil M. Ferguson
John S. Ma

July 1971

A B S T R A C T

Reinforced concrete inverted T-beams that support precast stringers on the flanges of the inverted T were studied in 24 load tests on 6 specimens. Results provide advice for reinforcement details and design procedures applicable to the flanges as well as the web shear strength of such beams.

S U M M A R Y

Beams constructed with a cross section in the form of an inverted T possess on each side of the web a shelf that provides a convenient supporting surface for precast members. Inverted T-beams are finding frequent use as bent cap beams to support stringers. The applications of load to the lower portions of concrete beams create tensile forces not ordinarily encountered in concrete construction. Reinforcement for the flanges of the T presents special problems regarding the shear strength, the anchorage of bars, and the flexural behavior in the flange or shelf.

Twenty-four load tests were conducted on six inverted T-beam specimens, in order to study reinforcement details, behavior, and mode of failure. The results of these tests have been compared with appropriate general theories and analytic estimates, and recommendations have been made for the design of such members.

(1) For concentrated reactions located at a distance 'a' from the face of the web, there must be adequate depth to sustain by shear friction (at $0.20f'_c$), acting on a width not more than 4a, the applied ultimate force.

(2) Within a width of 4a centered about concentrated loads, there must be enough steel passing through the web and into the brackets to develop the normal force required to maintain shear friction resistance using 1.4 for the coefficient of sliding friction in concrete.

(3) The effective width of shelf for bracket flexural calculations should be taken as 5a with a moment arm jd = 0.8d to support ultimate loads. Bracket flexural steel should be anchored by welding it to a longitudinal bar at the outside edge of the bracket.

(4) Stirrups for the web of inverted T-beams should be designed to carry all diagonal tension not assigned to concrete. Stirrups within a space equal to the depth of the web centered about a concentrated load must be able as hangers to support the

concentrated load. Web shear forces need not be superimposed on hanger forces, but the larger requirement for either can govern design. Since many shelf or bracket flanges are relatively shallow, hanger stirrups should be closed across the bottom of the web.

I M P L E M E N T A T I O N

The research reported here involved 24 physical tests on 6 reinforced concrete beams made to represent bent cap girders with a cross section in the form of an inverted T. Principal test loads were applied to the top of the shelf formed by the flanges of the inverted T in order to determine standards for the design of reinforcement in such beams. Specific recommendations for design are stated in the conclusions to the report.

One aspect of behavior not covered by this research project involves the probability for significant torsional loading on bent cap girders. All tests reported here involved the application of load simultaneously and in equal amounts on each side of the T-beam web. That loading represents a governing design condition for many cases, but in practice, every time traffic crosses such a bent cap, a reversal of torsion occurs. Torsional loading can govern some design conditions, particularly for bent caps with a stem more than 30 in. wide.

The most effective implementation of the results from this study would be realized through the distribution of the Conclusions chapter to bridge designers, both for immediate advice and for encouraging further considerations of refinements in design procedures.

C O N T E N T S

SHEAR AND ANCHORAGE STUDY OF REINFORCEMENT IN INVERTED T-BEAM BENT CAP GIRDERS

By

Richard W. Furlong, Phil M. Ferguson, and John S. Ma

I.

INTRODUCTION

Girders that are used as bent caps to support precast stringers must contain a flat surface to receive the bearings of stringers. If the stringers are simply placed on bearings at the top of the bent cap girders, the structural behavior of the girder is well-understood, and no special problems of reinforcement details are encountered. However, the elevation view of a bridge and the amount of headroom available beneath the bent caps can be improved considerably if the stringer bearings are placed on a shelf as shallow as is practical at the bottom of the girder. Bent cap girders with such a shelf on each side possess a cross section in the form of an inverted T.

Placing the shelf at the bottom of a girder web introduces some stress conditions that are not encountered in traditional practice with monolithic construction but which are unique to construction with precast concrete elements. In monolithic concrete construction, the girder web, stringer webs, and the deck slab would be cast at the same time. Stringer loads in monolithic construction are delivered directly through the stringer web and into the upper part of the girders where a combination of vertical compression stress and longitudinal flexural compression stress helps to reduce diagonal tension (shear) stress in the girder web. On the contrary in precast construction, placing the stringer reactions on a bearing plate

at the lower part of the girder web generates extra diagonal tension in the girder web.

The diagram in Fig. 1 will be used to help illustrate regions where stress conditions unique to inverted T-beams must be given special consideration. The increase of diagonal tension in the girder web, marked I in Fig. 1 has been mentioned already. The increased diagonal tension is closely related to a requirement for direct vertical tension capacity to support the shelf, called hanger tension and marked II in Fig. 1. Diagonal tension and hanger tension affect vertical web reinforcement (stirrups) in the girder, but shelf loads themselves must be delivered to the girder web by the shelf acting essentially as a bracket.

Bracket flexure is suggested near the symbol III in Fig. 1. Bracket behavior is about the same whether the bracket concrete serves the girder itself as part of the tension portion (positive moment region) or the compression portion (negative moment region) of the girder. However, bracket loads placed near the ends of the girder can create special problems due to the small twisting suggested by the bracket shear symbols at IV in two faces at the end of the member in Fig. 1.

The purpose of this study is to examine the behavior of inverted T-beams and to provide recommendations for their design. For a study of bracket behavior two essentially full scale specimens were constructed incorporating details and dimensions being used by the Bridge Division, Austin Office of the Texas Highway Department. Several different arrangements of bracket reinforcement were employed in the two specimens in order to determine good or bad effects from each arrangement. The two specimens revealed little or no anchorage strength problems that would be obscured by further testing of inverted T-beams of reduced size, and four additional specimens were constructed at one-third the scale of the first two specimens. The one-third scale specimens were used for studies of arrangements of girder web reinforcement and girder web strength, as well as additional studies of bracket behavior.

Analytic routines of various degrees of sophistication were employed both to interpret the results of tests and to project probable modes of behavior into a wider variety of design conditions. The internal distribution

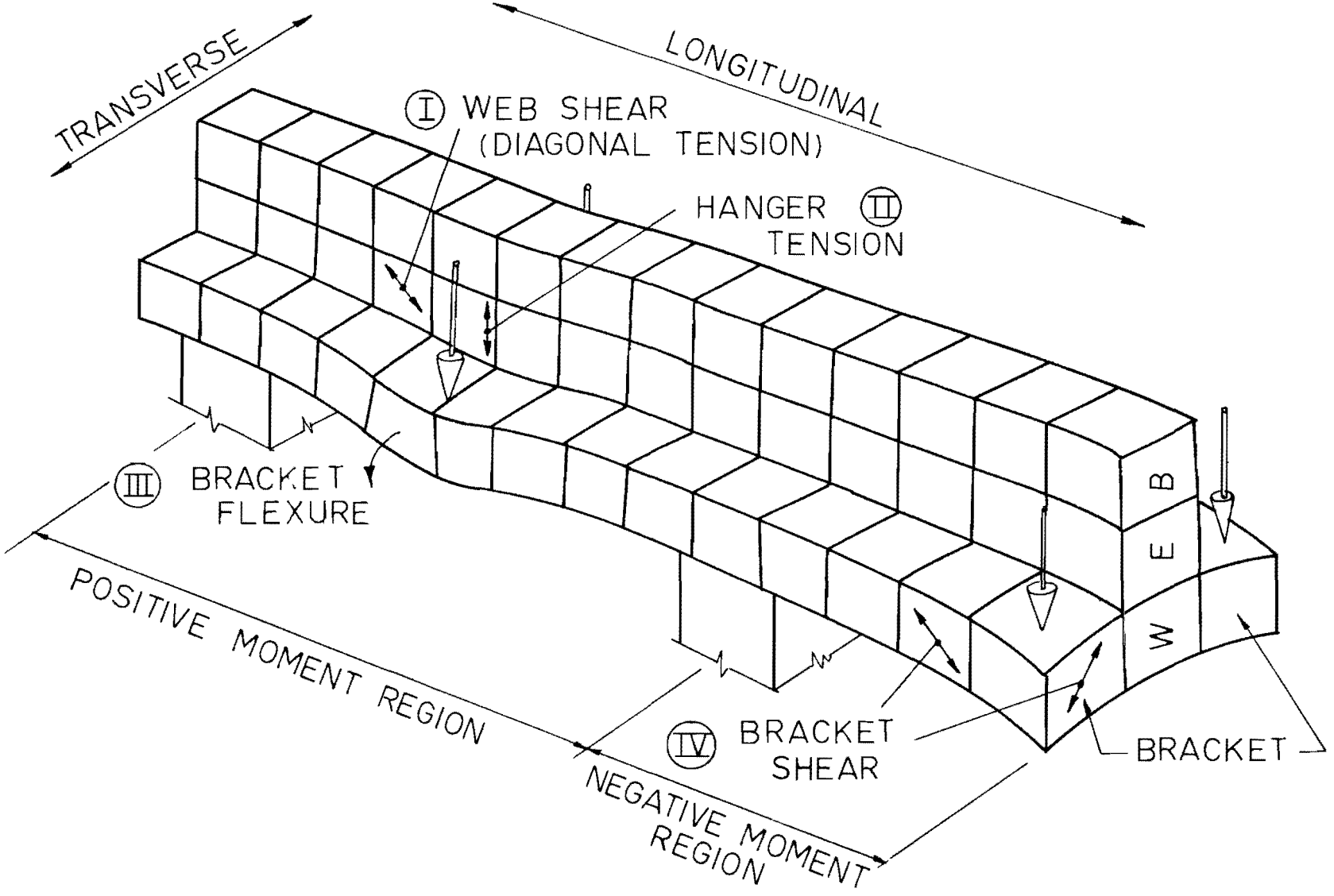

FIG. 1 INVERTED T-BEAMS

of forces within the inverted T-beams represented such a highly complex and statically indeterminate phenomenon that some analytic facility was a necessary part of data interpretation. Recommendations useful for the design of inverted T-beams are included in this report together with a discussion of the analytic and test results that led to each recommendation.

II.

PHYSICAL TESTS

To each of the six specimens several different load patterns were applied in order to study failure modes under varying conditions and locations of maximum load. A total of 24 specific tests were made, and failure occurred in 15 of the tests. Loading equipment was inadequate to produce complete failures in most of the full-scale specimen tests. All one-third scale model specimens, however, were loaded until failure took place.

The study reported here deals only with loads placed symmetrically and in equal magnitude on brackets each side of the web of the inverted T-beam. Such loading represents full live load on both spans supported by the inverted T-beam. Further study involving loads of different magnitude on only one side of the bracket and considerations of complications due to the resulting torsion are part of the subsequent project now underway.

Materials

Concrete. All specimens were made with Alamo Red Bag High Early Strength Type III cement. Fine aggregate consisted of Colorado River sand and coarse aggregate was Colorado River gravel passing a 1-1/2 in. sieve. In the one-third scale models all the coarse aggregate passed a 5/8 in. sieve. Proportions of the concrete mix by weight were 1:3.3:4.8 for the full-scale specimens and 1:1.8:3.5 for the one-third scale models. Usually the water/cement ratio was 6.0 gallons per sack for the full-scale specimens and 5.4 gallons per sack for the one-third scale models. Some adjustment of the quantity of water actually used was made in the field in order to maintain a consistent value of slump between 3 and 6 in. for all specimens. The compressive strengths of standard cylinders at the time of each test are listed in Table I. The strengths that are reported are obtained from an average of at least two cylinder tests. As shown in

TABLE I. COMPRESSIVE STRENGTH OF CONCRETE

Beam No.	Test	f'_c (psi)	Beam No.	Test	f'_c (psi)	Beam No.	Test	f'_c (psi)
B1	1	4087	BM1	1	4060	BM3	1	3740
	2	4100		2	4100		2	4030
	3	----		3	4100		3	4100
	4	4347					4	----
	5	----	BM2	1	4000			
	6	4680		2	4100	BM4	1	4250
				3	4420		2	4345
B2	1	3820		4	4630		3	4600
	2	4000						
	3	3800						
	4	3920						

Table I all of the recorded strengths were between 3740 psi and 4680 psi, representing a favorably small band of strength variations.

Steel reinforcement. All reinforcing bars were A-432 deformed steel reinforcing bars with a nominal yield strength of 60 ksi, except for a few intermediate grade #2 bars that were used in the model beams as ties in the bracket. A typical stress-strain curve for #3 bars of A-432 steel is shown in Fig. 2.

Electric resistance strain gages were attached to reinforcing bars in order to help determine the distribution of force within the reinforced concrete specimens. In order to attach the strain gages, one lug (sometimes more than one lug) on one side of the steel bar was ground locally to provide a smooth surface for the strain gage. The smooth area was cleaned with acetone and treated next with metal conditioner. Neutralizer was applied, and strain gages were attached to the prepared surface with BUDD GA-1 strain gage adhesive cement. Then the strain gages were waterproofed with a coat of Devcon rubber. During the setting time of the rubber coating, lead wires were soldered for the strain gages. After a thorough check of the attachments

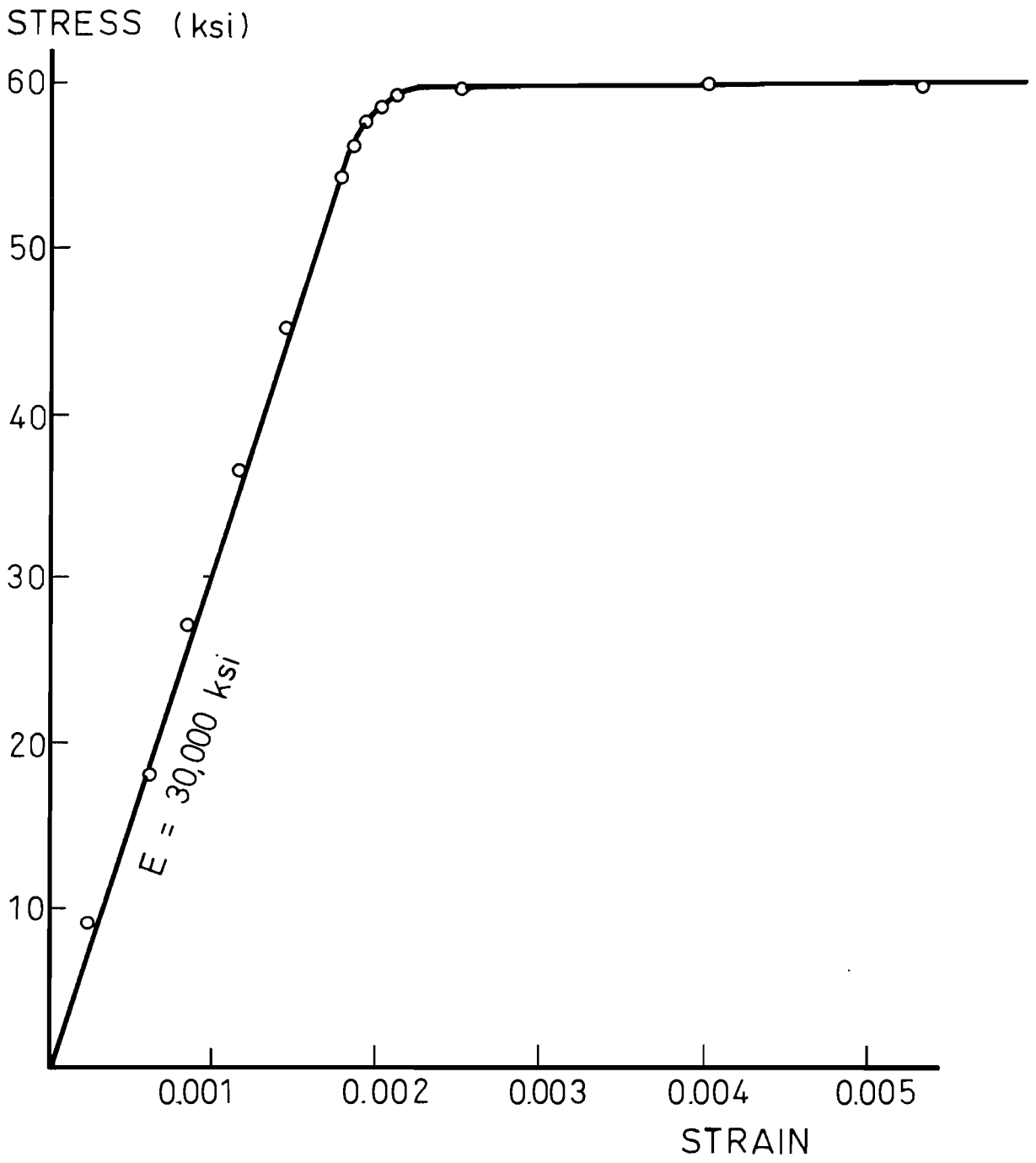

FIG. 2. STRESS-STRAIN CURVE FOR #3 A-432 STEEL

of each strain gage, lead wires were extended along the reinforcing bars and collected through embedded aluminum tubes to the outside of the formwork at convenient locations.

Casting and Curing Specimens

Cages of reinforcement were assembled in the laboratory. Bars were wired at intersections as much as possible in the same way as reinforcing cages would be assembled in the field. Wooden forms were used for all specimens, and form joints were taped inside to reduce water seepage. Forms were cleaned with air hoses and well-oiled before concrete was cast.

Concrete was placed in the form in lifts of approximately half the depth of the bracket. Several electric vibrators were used to obtain the desired amount of compaction of the mix into the form. Top surfaces were troweled to a smooth condition. Approximately 15 standard cylinders were cast with each specimen and cured under the same conditions as the specimen.

Specimens and cylinders were covered with cotton-filled curing mats that were kept moist during the first three to five days after the specimens were cast. After the curing mats were removed, the specimens were left to dry in the laboratory atmosphere until they were prepared for testing.

Each specimen was cast in one pour without using a cold joint at the level of the top of brackets. Some difficulty was encountered in efforts to obtain a smooth, honey-comb free surface at the top of the brackets. The technique of casting all of the concrete below the top of the bracket and then applying a wooden form across the top of the bracket was not altogether successful. In some areas where honeycomb voids did occur, surface concrete was added to the specimens after forms were removed. An epoxy binder was applied to the surfaces in order to achieve a desired adhesion between the new surface concrete and the underlying specimen concrete.

Test Arrangement and Test Procedures

A schematic diagram for a typical test setup is shown in Fig. 3. Photographs showing the test setup for a full-scale specimen and for a one-third scale model specimen are shown in Fig. 4. As indicated in Figs. 3 and 4,

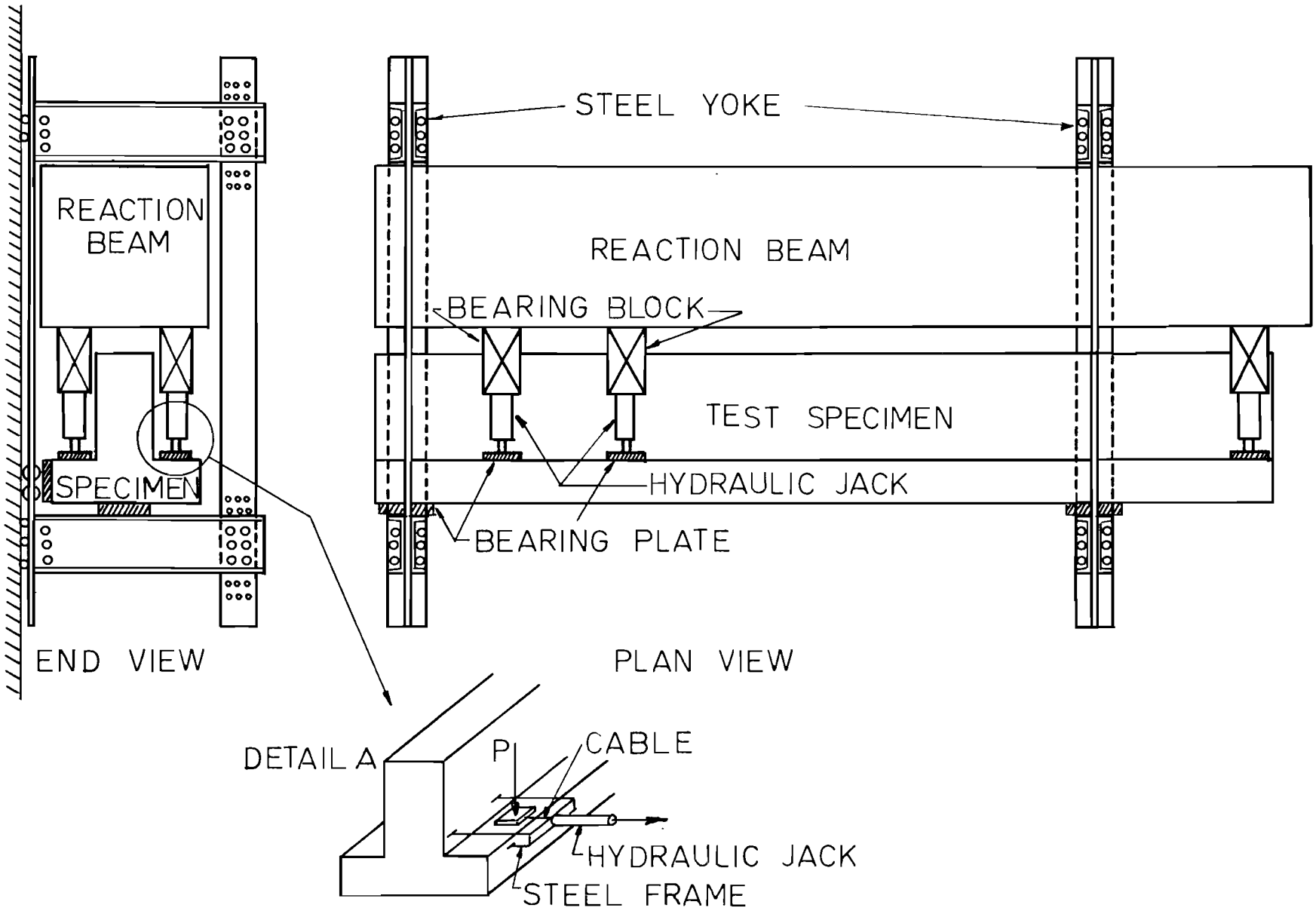

FIG. 3 TYPICAL TEST SET-UP

Full-Scale Specimen

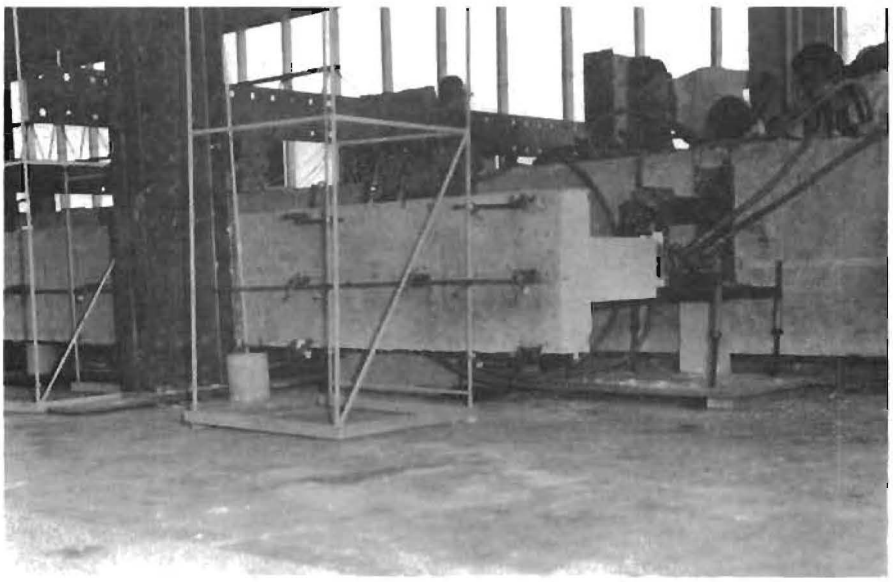

Model Specimen

Fig. 4. Photographs during tests

each beam was tested in a horizontal position with the bearing surface of the brackets in a vertical plane. The test specimens were supported on the lower side of one bracket by 6 in. diameter steel rollers bearing against steel plates. Bearing plates used at the reactions of test specimens represented columns in the actual bent cap structures. Test loads were applied by hydraulic jacks between the test specimen and a large reaction beam. In the two full-scale beam tests, 10 percent of the simulated stringer reaction was applied to the bracket in the test region perpendicular to the web of the specimen in order to simulate the longitudinal force that would occur due to stringer shrinkage or the longitudinal component of live load on a bridge deck. A detail of the horizontal force mechanism is shown in detail A of Fig. 3. The simulation of the longitudinal force was not adequate to represent a reaction from a bridge stringer, because the frame used to apply the force was too short. The simulation simply created a very local tensile stress that should have extended along the bracket at least as far as the effective bracket length for flexure. Data reported in subsequent sections indicated that the effective length was about 50 percent longer than the horizontal force bracket. No attempt was made to apply such a force in tests of the model specimens. No horizontal component of force was applied in the model beam tests which were directed more toward web behavior than to tension in flexural steel in the brackets.

For all tests of the full-scale specimen, neoprene pads 9 in. wide, 19 in. long, and 1 in. thick, were placed beneath steel bearing plates at each simulated stringer reaction. No neoprene pads were used in the one-third scale model beam tests, but instead steel bearing plates 4 in. wide, 1 in. thick, and 6 in. long were set in plaster of paris on the concrete bracket surface. The plaster provided a smooth stress distribution under the bearing plate.

Loads were applied in several increments until failure was approached or a capacity limit for the loading system was reached. Initially a load increment approximately 10 percent of the anticipated ultimate load was used until some indication of distress or actual failure was anticipated, at which time the load increments were reduced in order to approach a failure stage slowly. Readings taken at loads near the failure load were found to be the most meaningful in helping to describe the failure mechanism in the

test specimen. At each load increment, readings were made of strain gages on the reinforcing bars, and dial indicators were read to indicate the deflected shape of the specimen. Cracks that developed during the test were marked with pencil and the extension of cracks after each load increment was recorded. Cracks on the lower side of the beam could not be examined during the test. Crack patterns were examined after all tests of each specimen and the crack pattern was found to be very similar, almost symmetrical, each side of the centerline of the inverted T-beam.

III.

SPECIMENS AND TESTS

Full Scale Specimen 1

Figure 5 shows details of the reinforcement used for full-scale Specimen 1. This first specimen was intended primarily to study several different arrangements of reinforcement in the bracket. Horizontal bars in the top of the bracket were placed either at 3-in. centers or at 4-3/8 in. centers in different parts of the bracket. The diagonal bent bars marked L#6 were placed only in one load position for the bracket. The spacing of stirrups in the web of the specimen was usually 4-1/2 in. ($p_s = A_v/b's = 0.014$), but near the left-hand end of Specimen 1 the spacing was increased to 7-1/2 in. ($p_s = 0.008$) between pairs of #5 and #6 stirrups placed as bundled bars in the specimen. Stirrups marked J in Fig. 5 were left open at the bottom, and the open stirrups terminated 4 in. above the bottom of closed stirrups marked H.

Six loading arrangements were applied to the first specimen. Load positions for each test are shown by the numbers in Fig. 6, each number representing one load position. Loading for the first test was stopped at P = 310k on each bracket, because the electrical strain indicator had developed a malfunction. Loading for the second test was stopped also at P = 310k after a wide diagonal crack had appeared in the web near the left edge of the bracket where stirrups were lighter than those at the right edge. It was desired not to destroy the end of the specimen before further test loads could be applied. Loading for the third test was stopped when P reached 400k, the capacity of the loading system. The load of 400k each side of the web and 30 in. away from reactions generated a nominal web shear of 490 psi. Loading of test 4 reached P = 380k when one of the loading pumps developed a leak. Loading of test 5 again reached the capacity of the rams at P = 400k. The fifth test was a repeat of the test arrangement used for the first test which had been stopped at a load of 310k. A load of 400k was applied in the fifth test with no indication of failure. Test 6 finally developed a shear failure at a load of 380k, the failure due to bracket shear-off occurring near the right support of the specimen. The shear stress obtained by

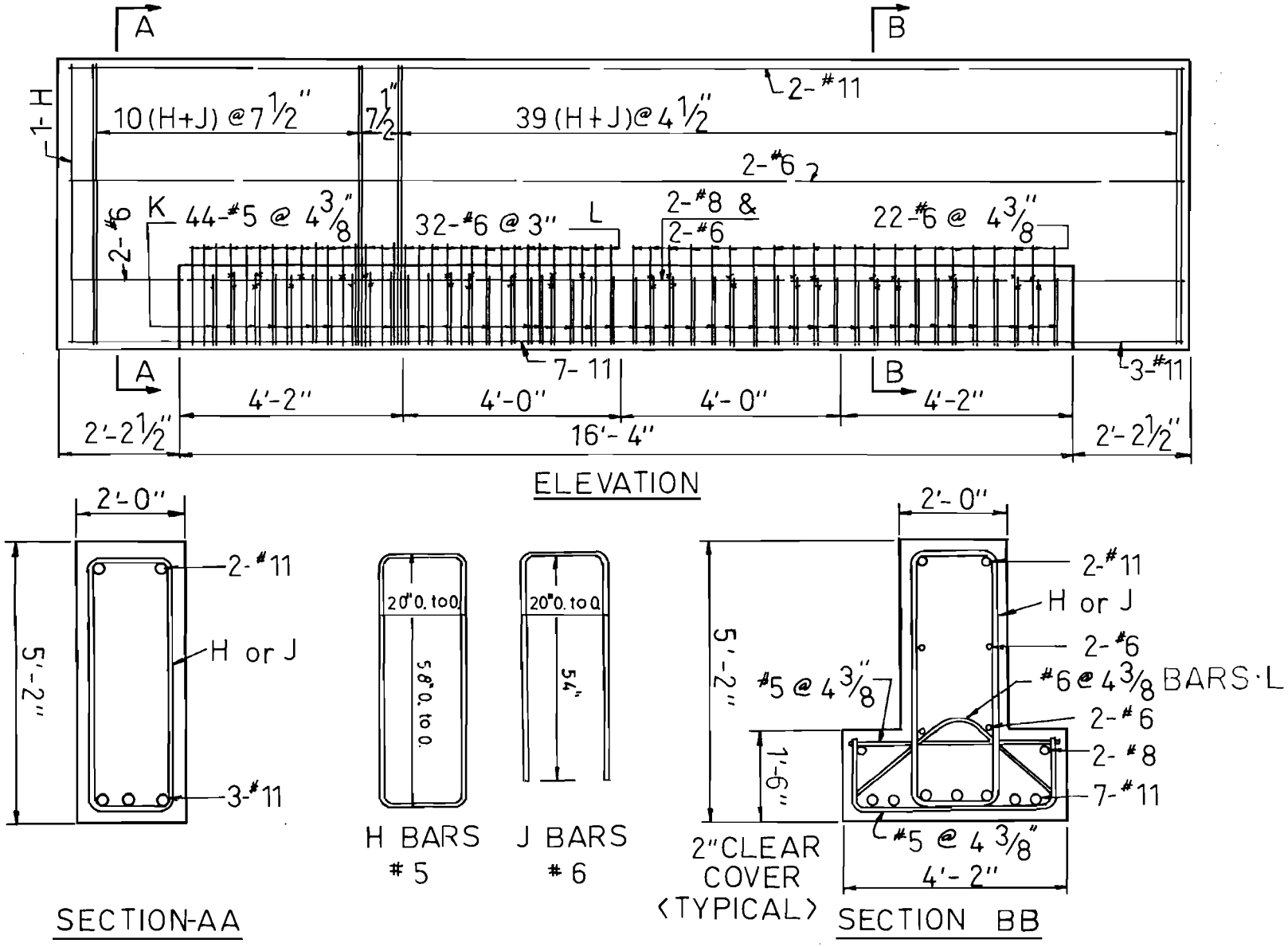

FIG. 5 DETAILS OF FULL SCALE SPECIMEN 1.

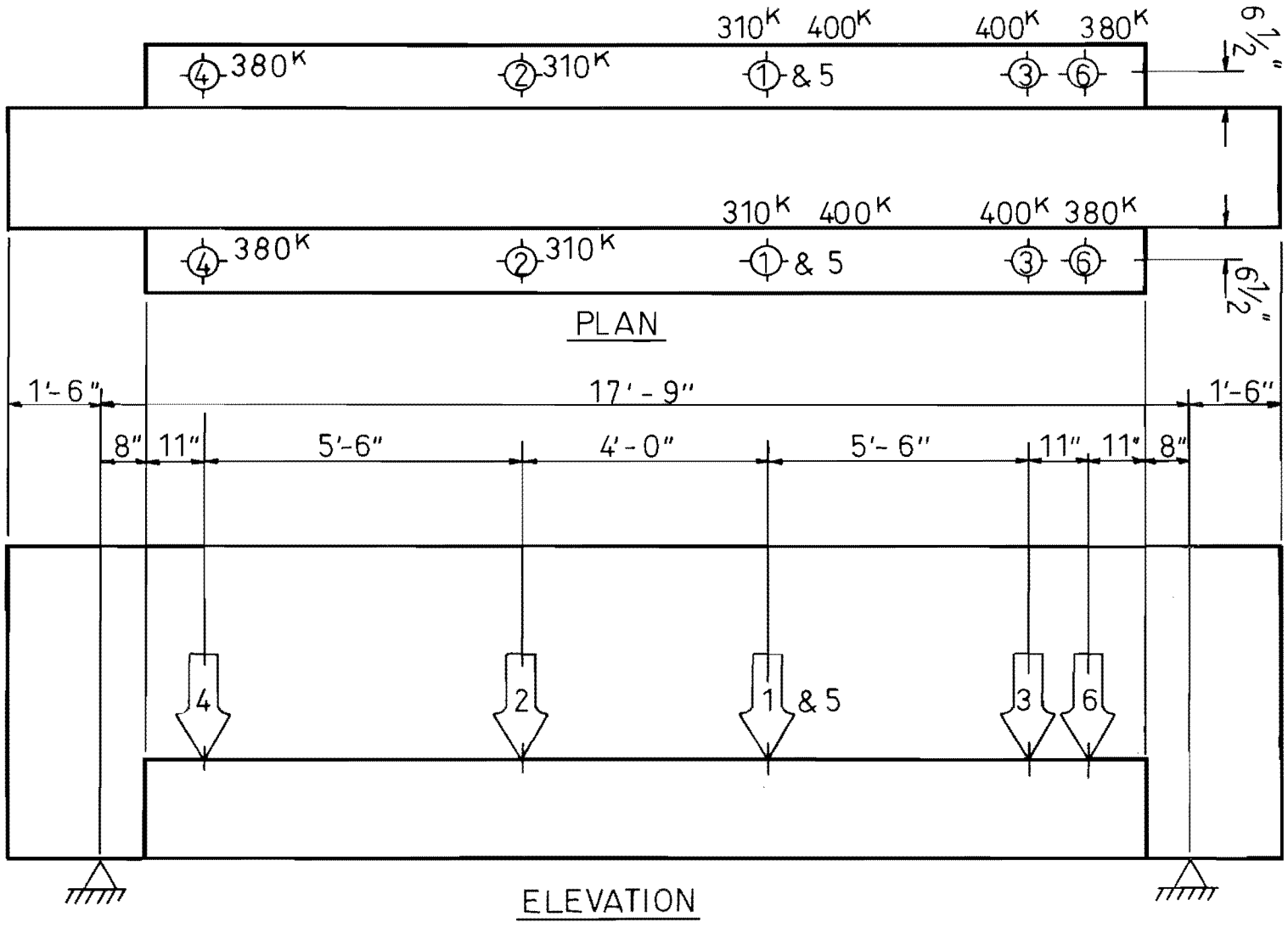

NUMBERS REPRESENT SEQUENCE OF LOADING. MAXIMA SHOWN IN PLAN VIEW

FIG. 6. LOAD POSITIONS FOR FULL SCALE SPECIMEN 1.

dividing the failure load by the area of the sheared-off face of concrete was 1.10 ksi.

Strain gages on the reinforcement indicated that the inclined bars were more active than the horizontal bars in resisting flexural tension in the top of the bracket. In test 6, a wide diagonal crack that developed in the web near the right reaction of the bracket indicated that the inverted U open stirrups had failed to function effectively as hangers at high load after anchorage at the lower end of the stirrups had been lost. Strain gage readings showed that the closed stirrups in the same region had reached their yield strength.

Full Scale Specimen 2

Figure 7 displays the reinforcement details used for the second full-scale specimen. The second full-scale specimen was constructed with a bracket 15 in. deep, 3 in. shallower than that used for Specimen 1, but with the same 18-in. width. Bracket flexure was resisted only by horizontal bars in most of Specimen 2. Diagonal bars were used in the bracket for only one-fourth the length of the bracket, and the area of horizontal flexural steel in the bracket was correspondingly reduced in the region with the diagonal bars.

Stirrups open at the bottom were used in the second specimen, much the same as in the first specimen, each bundled next to a closed stirrup. Since the bracket was shallower for the second specimen, anchorage problems at the bottom of the open stirrups were anticipated. The open legs of the bars were 3 in. shorter than the distance to the bottom of the closed stirrups. Strain gages were mounted on both closed and open stirrups at the level of the top of the bracket.

Four load positions were examined on this specimen. The load positions are shown in Fig. 8. In the first test strains measured on the stirrups located 3 in. from the left end of the bracket indicated that the open stirrup developed slightly higher strains than did the closed stirrup before the load had reached 212k. For loads greater than 212k, the open stirrup showed decreasing strains, while the closed stirrup continued to develop higher strains. The loss of strain in the open stirrup indicated a loss of bond anchorage at its open end, and showed rather clearly that the anchorage of

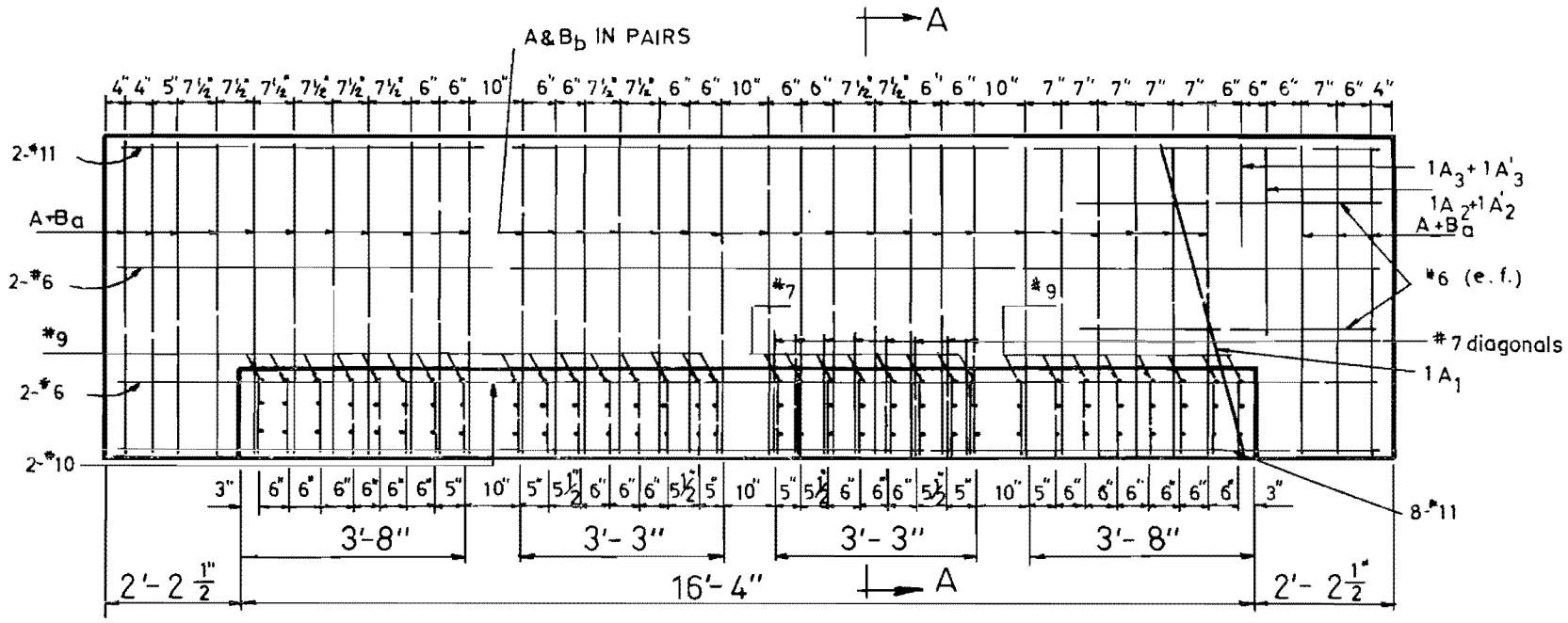

ELEVATION

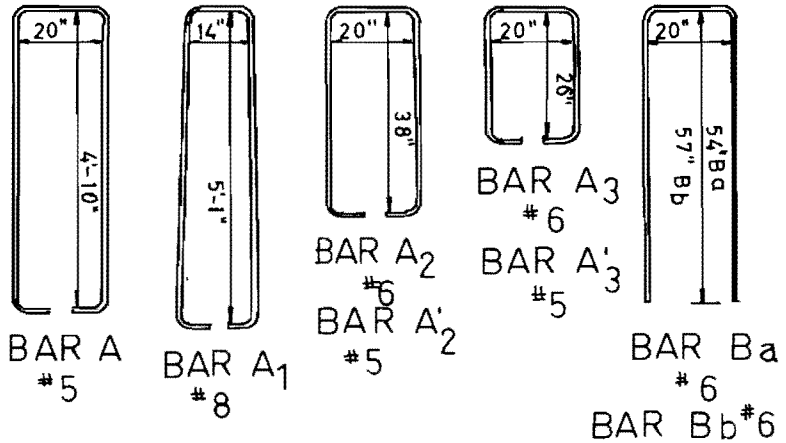

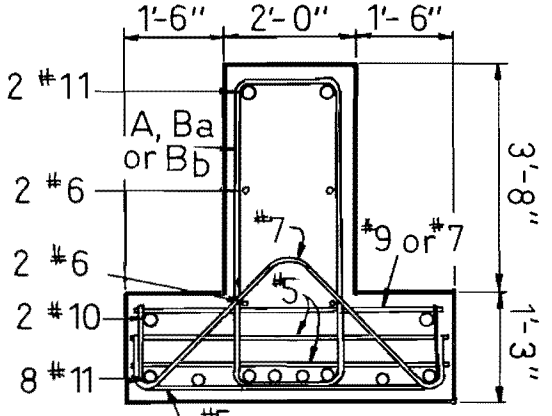

SECTION AA

FIG. 7- DETAILS OF FULL-SCALE BEAM 2.

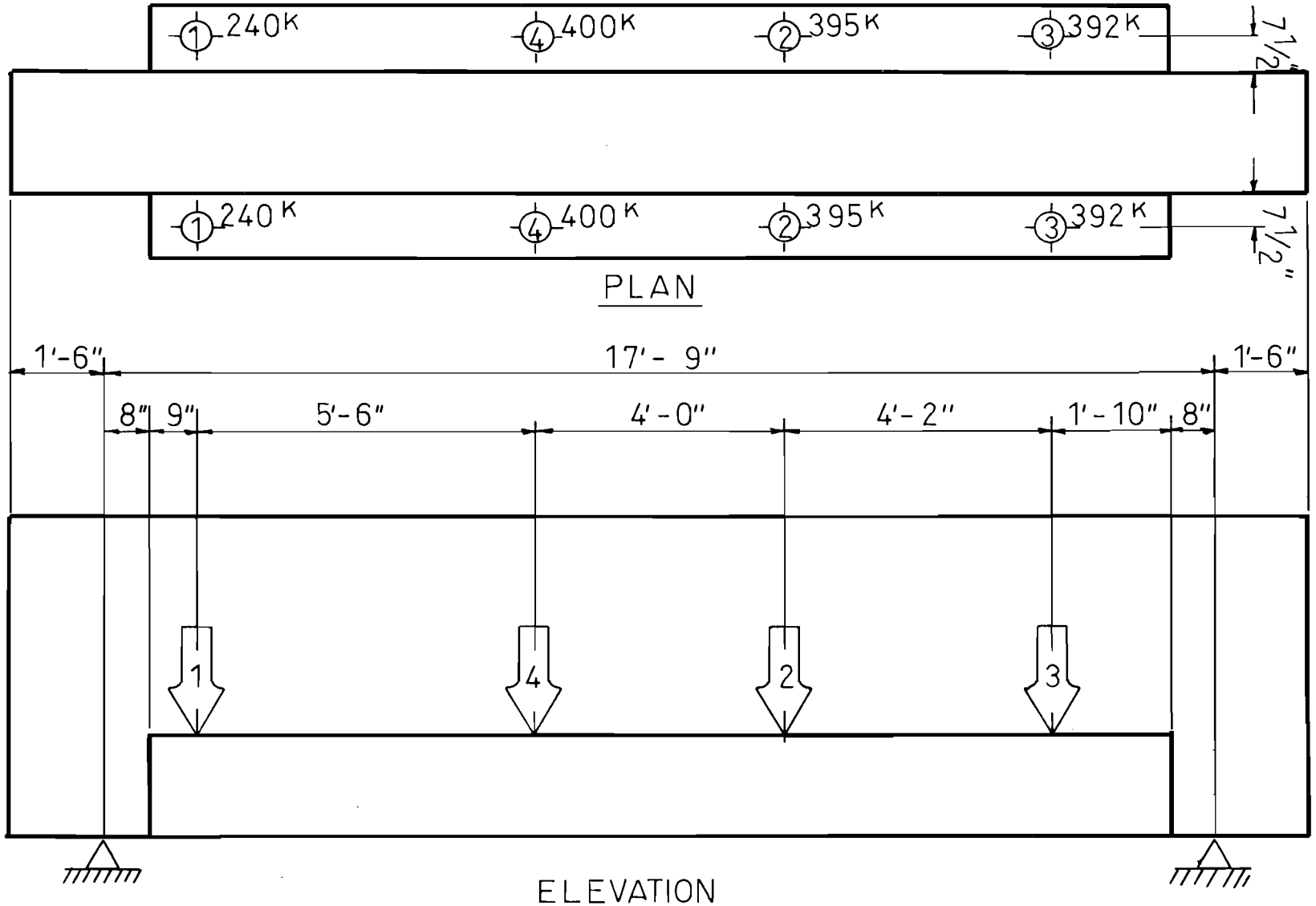

NUMBERS REPRESENT SEQUENCE OF LOADING MAXIMA SHOWN IN PLAN

FIG. 8. LOAD POSITION FOR FULL—SCALE SPECIMEN 2

closed stirrups around longitudinal steel is a necessary mechanism in order that stirrups can act effectively as hangers to deliver the bracket loads into the upper part of the inverted T-beam web. Loading for the first test was stopped at P = 240 kips and a nominal web shear stress of 314 psi, after a 1/4-in. wide diagonal crack in the web near the left end of the beam had formed.

Loading for test 2 was carried all the way to P = 395 kips, the full capacity of the loading system. The principal load for test 2 was in the region which had diagonal bars as well as horizontal bars in the bracket. Strain gage readings indicated that the diagonal bars, in contrast to those in the 18-in. deep bracket of Specimen 1, were less effective in resisting bracket flexure than the horizontal flexural bars. The diagonal bars were placed only in the region of test 3 on this specimen with 15-in. thick brackets.

Loading for tests 3 and 4 extended to the full capacity of the loading system near 400 kips in both cases. Anchorage at the end of the open stirrups was adequate to develop yield strain in some of the stirrups that extended farther below the top of the bracket than those which failed to develop yield forces near the left end of the specimen. It is possible that if the applied force had been extended above 400 kips, some anchorage problems in the open stirrups could have developed at the higher level of load. It seemed apparent that closed hangers anchored around longitudinal flexural steel at the bottom of the inverted T-beam always had the capability to develop the full yield strength of the stirrup.

Model Beam 1

Reinforcement details and dimensions for Model Beam 1 are shown in Fig. 9. The first model beam was designed to reveal characteristics of web shear in the inverted T-beam, and all model beams had "shallow" brackets 6 in. wide and 6 in. deep similar in shape to full-scale Specimen 2. Three load arrangements were applied to this specimen. The first load arrangement, shown in Fig. 10, involved a test in which the bracket part of the beam was in compression, as the load was applied to a portion of the beam cantilevered beyond one of the reactions. The second load arrangement and the third load arrangement involved loads applied to the bracket between the supports to

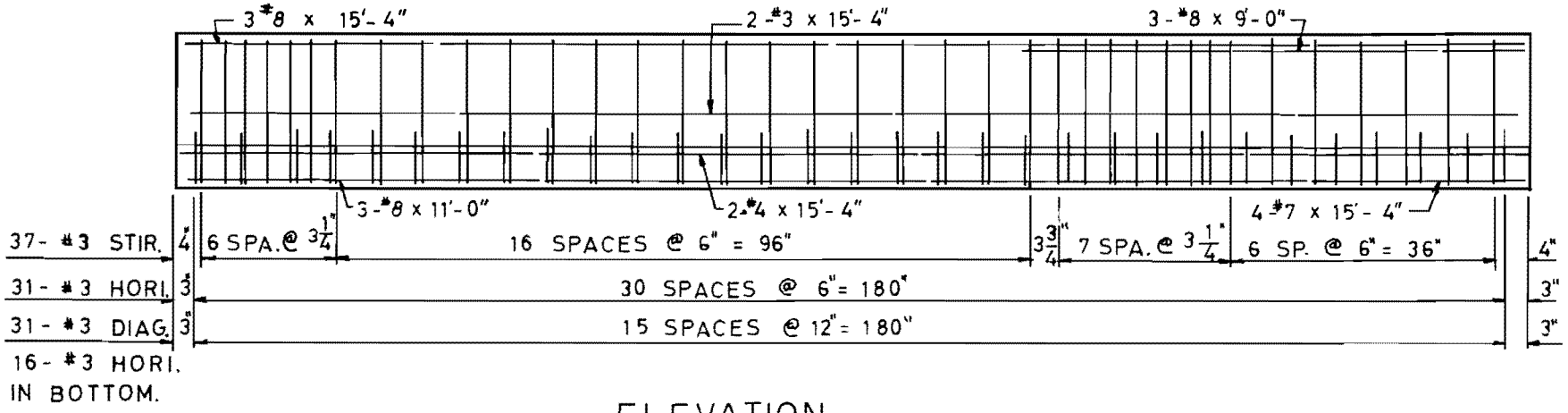

ELEVATION

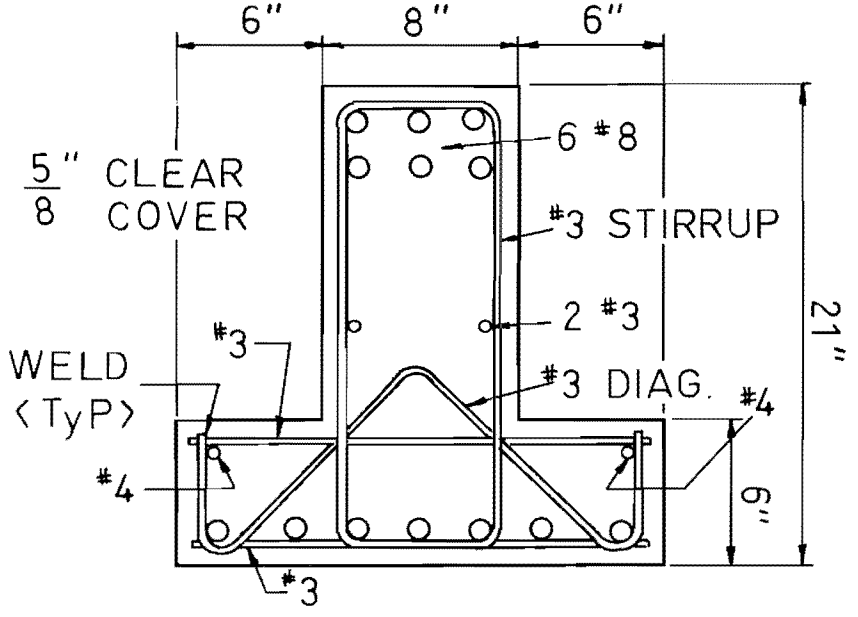

TYPICAL SECTION

FIG. 9 DETAILS OF MODEL BEAM 1.

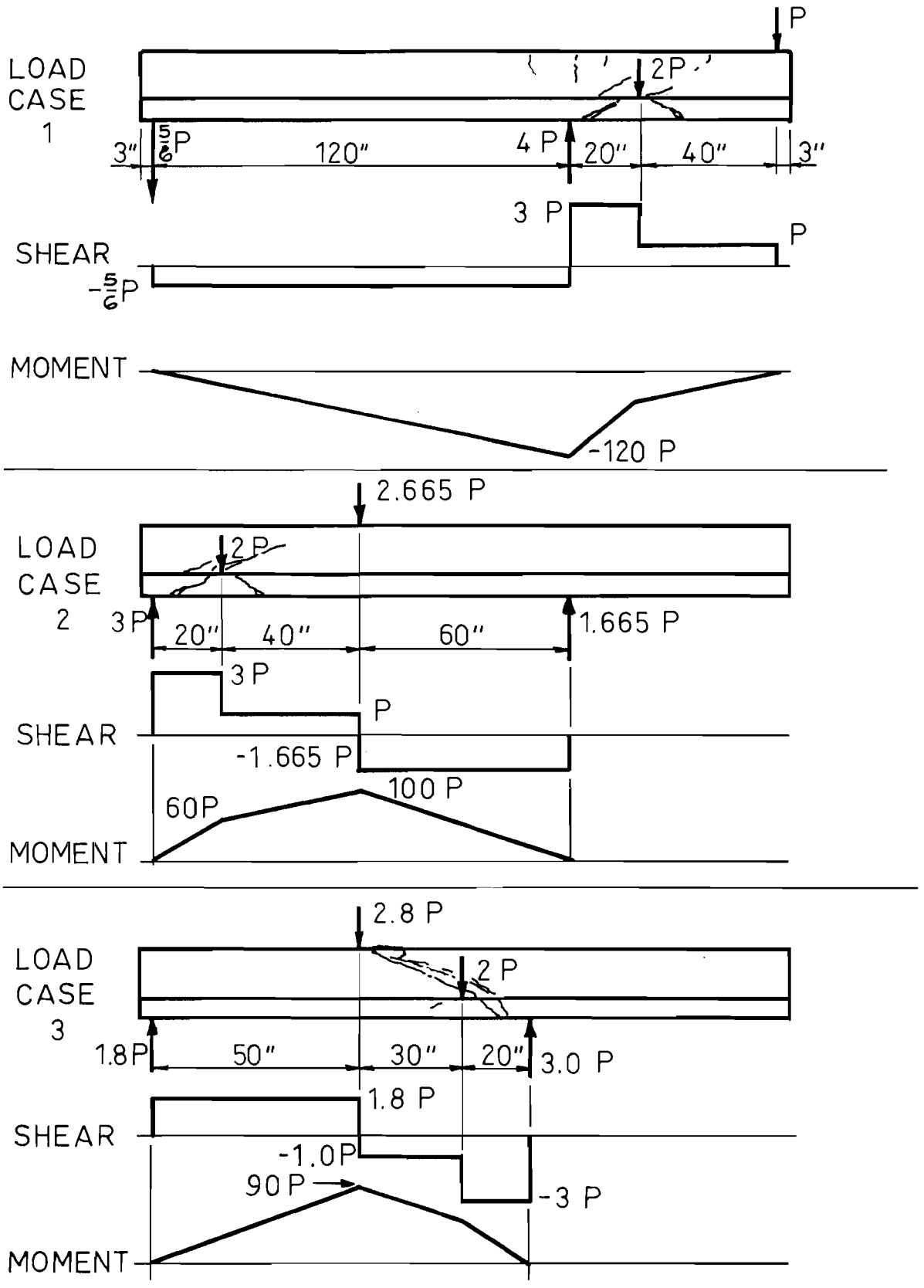

FIG. 10 LOAD ARRANGEMENTS FOR MODEL BEAM 1

the inverted T-beam, such that the bracket itself was a part of the tension region of the inverted beam. In all cases the position and the magnitude of loading were so arranged that the highest shear in the member would be equal to 3P. Stirrup spacing was made 3-1/4 in. ($p_s = A_v/b's = 0.0085$) for most of the specimen, but a spacing of 6 in. ($p_s = 0.0046$) was used in the high shear region for the third load position. Bracket reinforcement was identical for all parts of the specimen.

For the first load position with large forces applied at the center of the bracket (a = 3 in.) near the end of the bracket, a punching-flexure type failure occurred at a load P = 41k ($v_{max} = 0.79$ ksi). Sketches of major cracks at failure are shown in Fig. 10. The second and third load arrangements caused failure in the web of the inverted T-beam, essentially failures of a shear-compression type at loads P = 46.7 kips ($v_{max} = 0.90$ ksi) in the second load arrangement and P = 38 kips ($v_{max} = 0.73$ ksi) in the third load arrangement for which the stirrup spacing in the high shear region was wider. In both cases the ultimate shear compression failure occurred near the interior load where the M/Vd ratio was near 5.

Model Beam 2

Reinforcement details for Model Beam 2 are shown in Fig. 11. Loading arrangements used for each test and major failure cracks are shown in Fig. 12. Loading arrangement 1 (test 1) involved a study of maximum loads on a short overhang in which web stirrups were spaced at 3-in. centers ($p_s = 0.0092$) and horizontal bracket flexural bars were spaced at 2-in. centers. The second load arrangement also involved an overhang for which the span was longer than in test 1. Tests 3 and 4 involved the positive moment region of the inverted T-beam. The position and magnitude of loading were adjusted for tests 2, 3, and 4 such that the highest shear in the member would be equal to 3P. The highest shear for the first load arrangement was only 2P, and the corresponding M/Vd ratio was 0.8.

The first load arrangement created failure in the bracket with a punching-flexure twist type failure at P = 29k ($v_{max} = 0.37$ ksi). Failure in the second load arrangement began in the web with a wide diagonal tension crack before the final failure occurred in the bracket with another

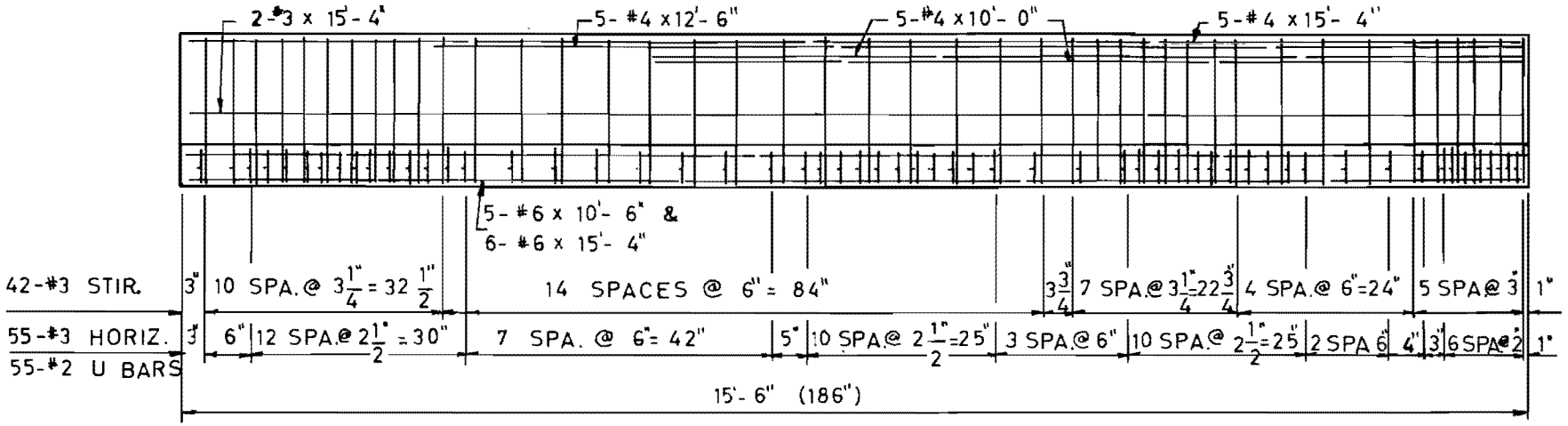

ELEVATION

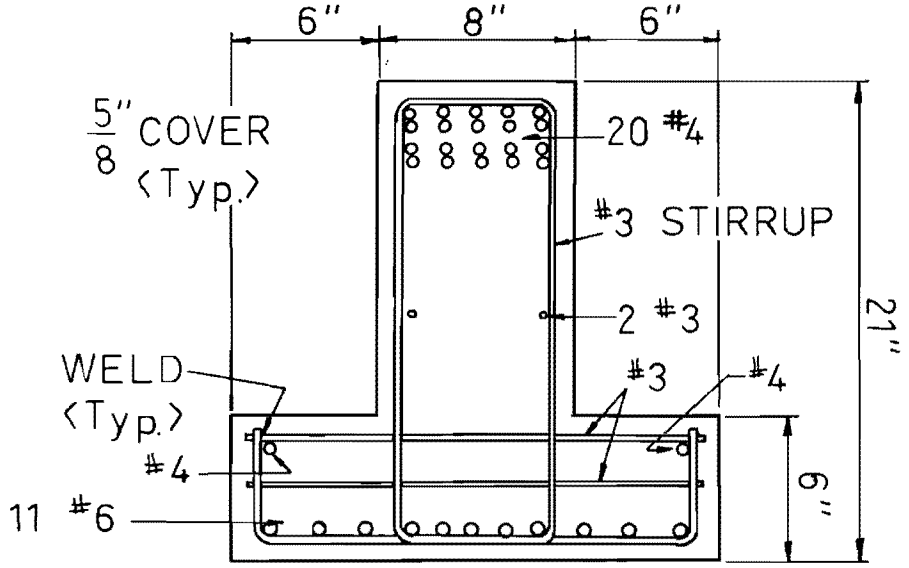

TYPICAL SECTION

FIG. 11 DETAILS OF MODEL BEAM 2.

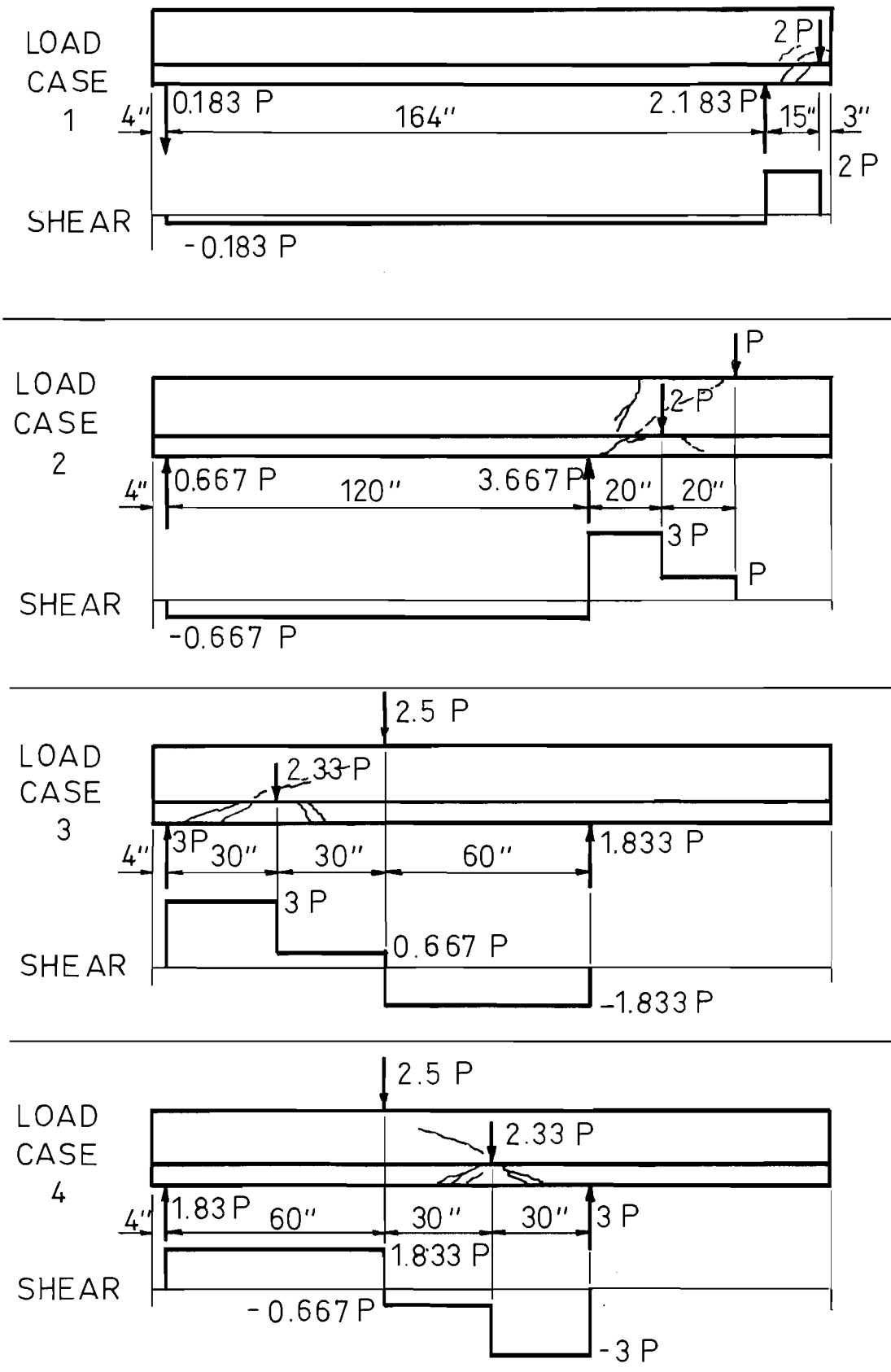

FIG. 12 LOAD ARRANGEMENTS FOR MODEL BEAM 2

punching-flexure and web shear type failure at P = 50k (v_{max} = 0.96 ksi). The bracket again failed with a punching-flexure-twist type failure at a slightly higher load of P = 51k (v_{max} = 0.98 ksi) in test 3. In test 4 hangers yielded at the bracket load before the final failure occurred, again in the bracket with a punching-flexure and twist type failure at P = 49k (v_{max} = 0..94 ksi).

Model Beam 3

Specific reinforcement details for Model Beam 3 are shown in Fig. 13, and the loading arrangement for each test is shown in Fig. 14. Model Beam 3 was intended to reveal hanger behavior because the yielding of hangers had been observed in Model Beam 2. Four test arrangements were used for Model Beam 3 with all loads applied at the top of the bracket, whereas some of the loads had been applied to Model Beams 1 and 2 at the top of the web. Load arrangements for tests 1 and 4 involved overhanging portions of the inverted T-beam, and the second and third load arrangements involved the positive moment region of the T-beam. Horizontal flexural bars in the bracket were spaced uniformly at 3-in. centers throughout the specimen. The 3-in. spacing for previous brackets had involved no apparent flexural distress in the brackets. The spacing of stirrups was either 6 in. (p_s = 0.0046) or 4 in. (p_s = 0.0069) in various regions of Model Beam 3. Test 1 involved a shear compression mode of failure in the web of the T-beam at a load P = 41.2k (v_{max} = 0.79 ksi). Failures in tests 2 and 3 initiated through yielding of stirrups before the final failure occurred in the web, again in a shear compression mode at P = 42.5k (v_{max} = 0.82 ksi) for test 2 and P = 43.5k (v_{max} = 0.84 ksi) in test 3. Failure in the fourth test occurred in the brackets with a secondary punching-flexure-twist type failure at P = 32.3k (v_{max} = 0.41 ksi) after all of the hangers in the overhanging region had yielded.

Model Beam 4

Reinforcement details for Model Beam 4 are shown in Fig. 15, and the arrangement of loads for each test is shown in Fig. 16. Only three tests were performed on Model Beam 4. Horizontal flexural steel in the bracket was

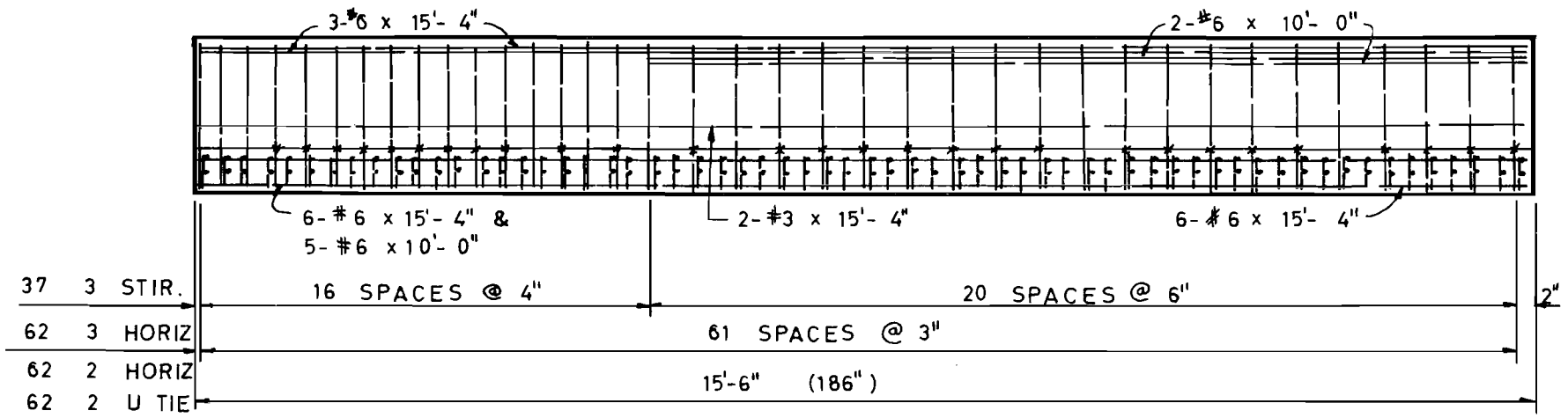

ELEVATION

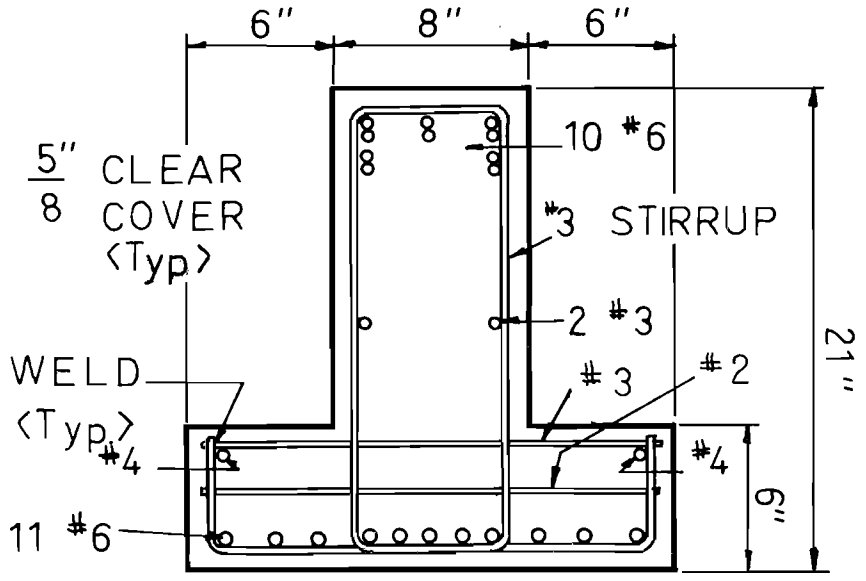

TYPICAL SECTION

FIG. 13 - DETAILS OF MODEL BEAM 3.

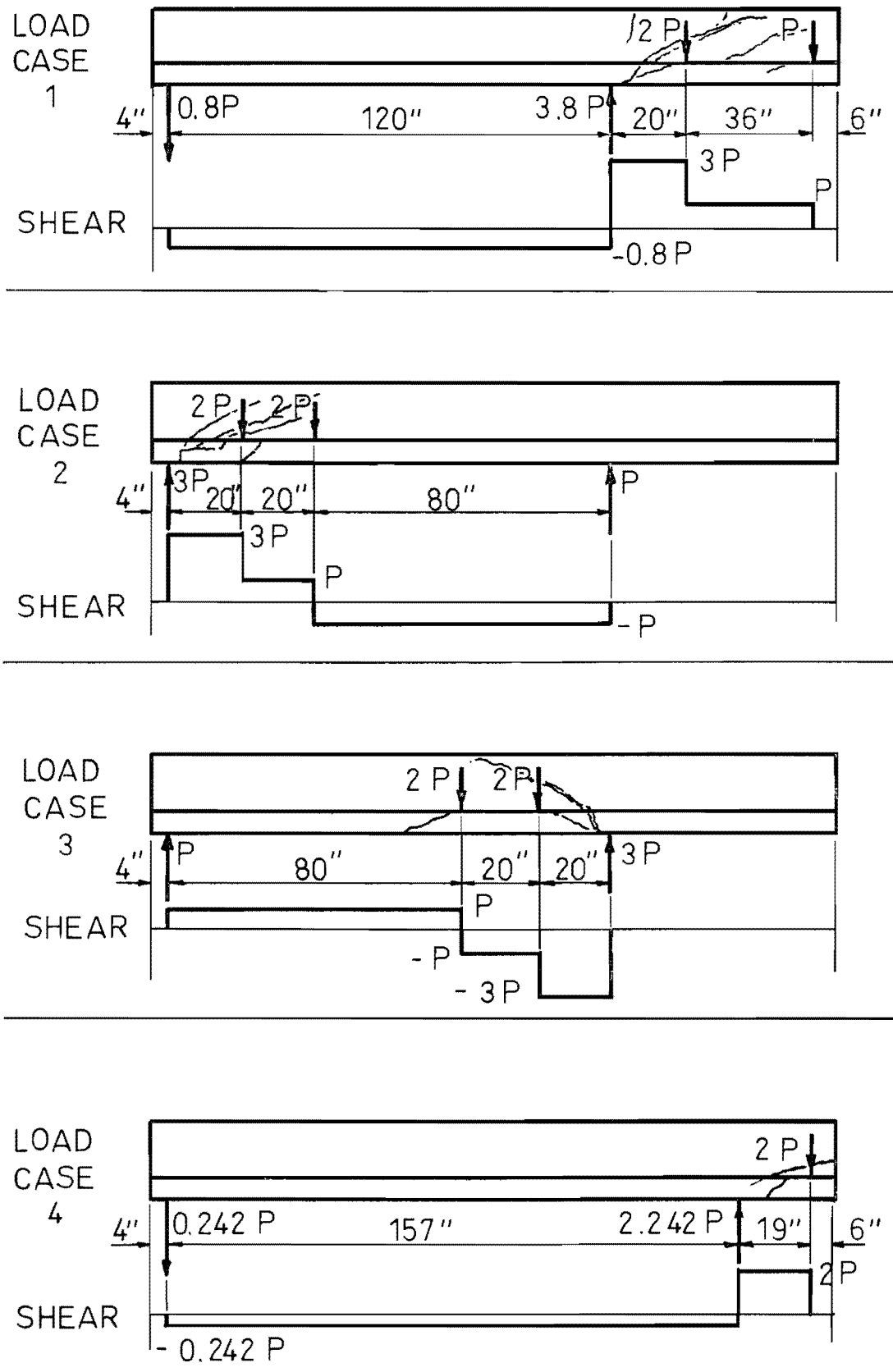

FIG. 14 LOAD ARRANGEMENTS FOR MODEL BEAM 3

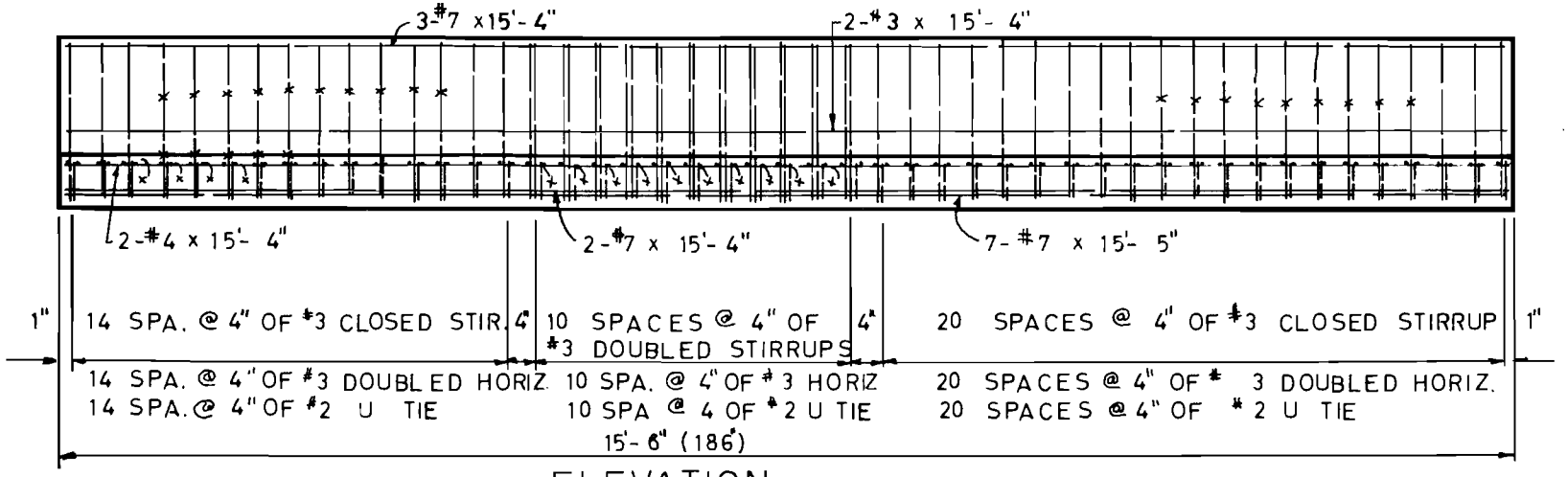

ELEVATION

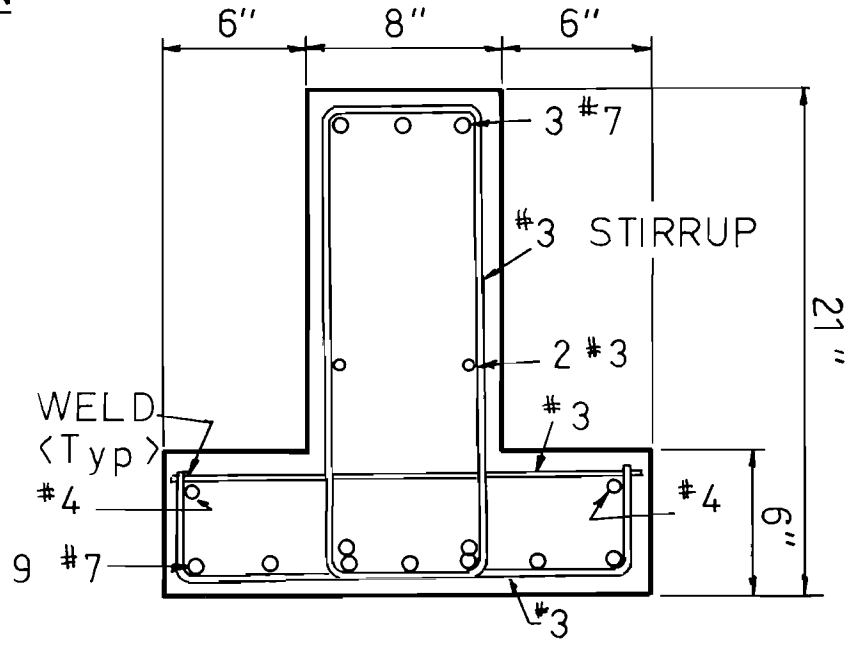

TYPICAL SECTION

FIG. 15 - DETAILS OF MODEL BEAM 4.

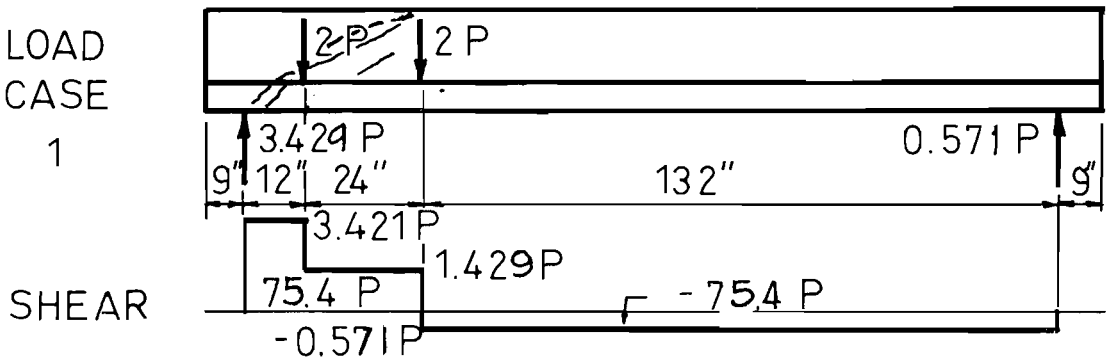

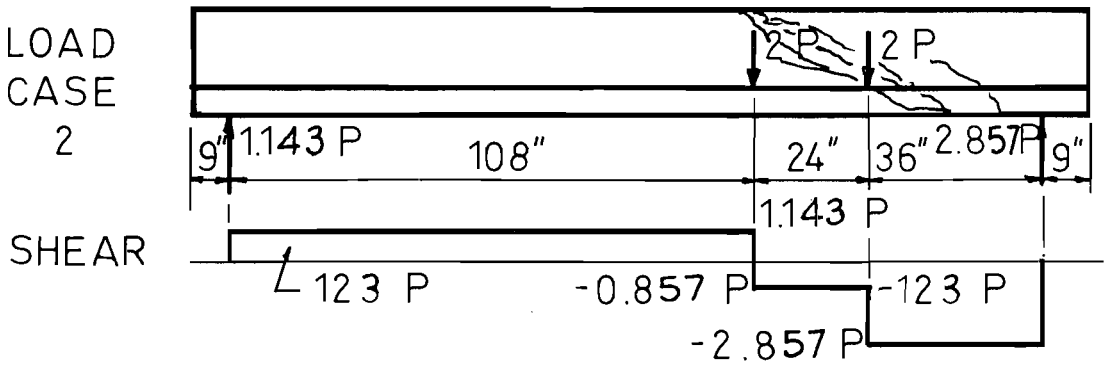

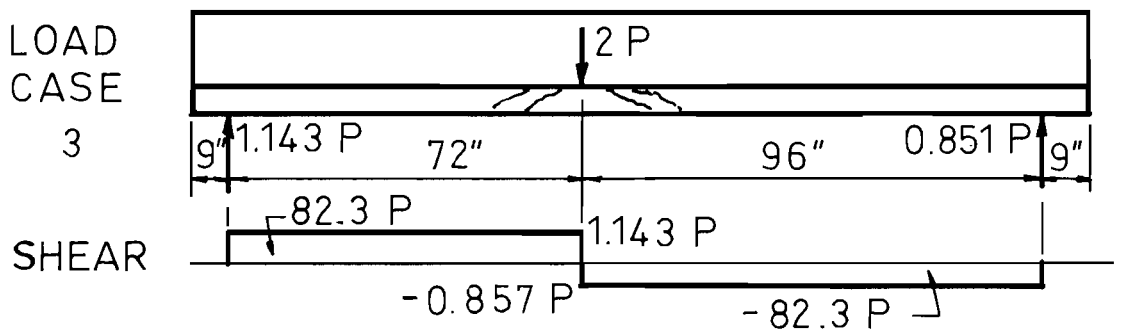

FIG. 16 LOAD ARRANGEMENTS FOR MODEL BEAM 4.

spaced only 2 in. apart in Model Beam 4 for regions of high load in tests 1 and 2. Stirrup spacing, for the same regions in tests 1 and 2, was 4 in. The third test was intended to reveal the distribution of bracket moments along the beam axis. Heavy stirrups (#3 in pairs @ 4 in. to provide p_s = 0.0137) were placed in the regions of high load for test 3 in order to prevent premature failure due to stirrup or hanger yielding. Horizontal flexural steel at the top of the bracket was spaced at 4-in. centers in the region of high load for the third test. All three tests performed on Model Beam 4 were made in the positive moment region of the inverted T-beam.

The first load arrangement involved a diagonal tension type cracking in the web before final web shear failure occurred, accompanied by bracket punching-flexure type failure at P = 48k (v_{max} = 0.92 ksi where M/Vd = 0.6). The second load arrangement created a typical shear-compression type failure in the web of the T-beam at P = 47.5k (v_{max} = 0.91 ksi where M/Vd = 1.8). A typical shear-compression type failure was characterized by crushing of compression concrete after a diagonal shear crack had propogated into the upper region of the web almost directly above the point of application of the load in the maximum moment region. The third test created failure in the bracket with another punching-flexure type failure at P = 53.8k (v_{max} = 0.40 ksi where M/Vd = 3.7) after a wide crack had opened at the face of the web indicating yielding of some horizontal flexural steel at the top of the bracket.

IV.

FAILURE MODES OF TEST SPECIMENS

Table II contains a summary of the specimen designation numbers and numbers of tests run for each specimen. After each test there is an indication of the type of failure that was observed for that test. As the tabulation indicates, more than one general type of failure was involved in some of the loading arrangements in one or more tests. The principal classification of failures could be divided into two categories, those involving failure essentially in the bracket or those involving failure essentially in the web of the specimen. Bracket failures were attributed either to shear friction or to flexure, always accompanied by punching shear complications

TABLE II. FAILURE MODES OF TEST SPECIMENS

Beam No.	Shear-span to Depth Ratio		Type of Beam	Bracket Failure		Hanger Failure	Web Shear Failure	
	Bracket	Beam		Shear-friction	Punching-flexure-torsion		Shear-compression	Shear-off compression zone
B1 - T1	0.425		Simple					
2	"		"					
3	"		"					
4	"		"					
5	"		"					
6	"		"	x				
B2 - T1	0.626		"					
2	0.637		"					
3	0.649		"					
4	0.432		"					
BM1- T1	0.626		Cant.		x			
2	"		Simple				x	
3	"		"				x	
BM2- T1	0.626	0.81	Cant.		x			
2	"	1.07	"		x			*
3	"	1.61	Simple		x			
4	"	1.61	"		x	*		
BM3- T1	0.600	1.11	Cant.				x	
2	"	1.02	Simple			*	x	
3	"	1.02	"			*	x	
4	"	1.06	Cant.		x	*		
BM4- T1	0.600	0.61	Simple		x			*
2	"	1.83	"				x	
3	"		"		x			

*Specimens failed in mixed modes and this sign indicates only that this failure mode appeared first during test.

longitudinally in the bracket. Web failures involved shear compression type failures or together with punching through the bracket, failure of stirrups acting as hangers to support the forces on the bracket.

Shear-Friction Failures in the Bracket

A shear-friction failure is one in which the concrete fails by sliding or shearing along the plane represented by the vertical face of the web of the inverted T-beam. In the short bracket it would be impossible to develop a shear failure because of diagonal tension, but at the face of the web of the T-beam failure would involve the pure shear strength of the concrete itself. Shear friction failure was observed for only one test during the study reported here. That test was the sixth load arrangement on full-scale Beam 1. Figure 17 contains photographs taken at the end of the specimen after the shear-friction failure. Note the displacement along the face of the web.

During the application of the sixth load arrangement to Beam 1 there was little sign of distress until the load reached 270k. (Loads throughout discussions reported here will refer to the force on only one side of the bracket.) As the load was increased above 270k the concrete cover on one face of the top bracket appeared to separate from the steel. A strain gage on the flexural steel in the bracket indicated 87 percent of the yield strength in the bar. At a load of 310k the yield strength of the flexural steel in the bracket was reached, and the strain gage on a diagonal bar indicated the diagonal bar had developed 70 percent of its yield strength. When the load reached 380k, the side cover on the opposite bracket also tended to move away from the steel. Efforts were made to maintain the load continuously on the bracket by pumping fluid into the rams. Load was maintained for about 10 minutes until the rate of deformation exceeded the capacity to extend the jacks. Eventually the concrete cover across the bottom of the beam broke free, as shown in Fig. 17(b).

Punching-Flexure Failure in Brackets

Punching failures of reinforced concrete members are generally associated with the design of footings to sustain concentrated load.

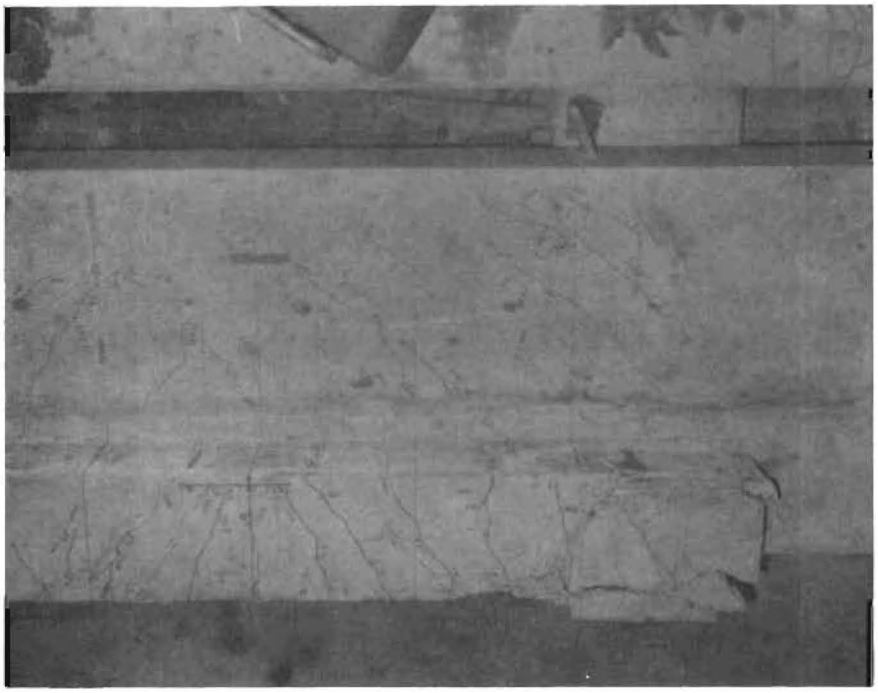

(a) Side View

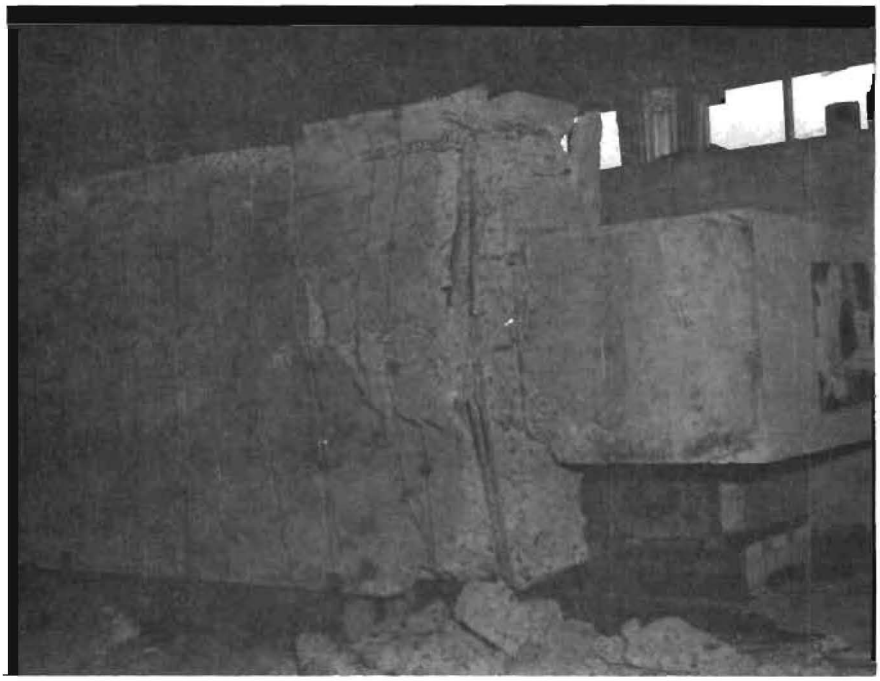

(b) Bottom View

Fig. 17. Failure pattern of Beam 1.

Punching failures involve a shear and diagonal tension separation along a truncated pyramid around a concentrated load. Punching failures were distinguished here from flexural failures in the bracket by the lack of crushing in the compression zone at the bottom of the bracket. When crushing occurred in the compression zone at the bottom of the bracket, the failure was said to be a flexural failure.

Eight of the load arrangements used in this study resulted in punching-flexure failures. A visible element of twist was involved with several of these failures. A diagram in Fig. 18 illustrates the propagation of cracking usually observed in punching-flexure failures. At loads of 30 percent of ultimate load P_u, a horizontal crack could be observed behind the loading plate at the top of the bracket along the web. These cracks were due to a combination of flexural bending stress and vertical tension or shear stress. This stage of cracking is marked by the numeral 1 in Fig. 18. After the initial crack had extended to a distance equal to the width of the bearing plates (sometimes a little longer), the cracks turned at an angle of roughly 45° to the web. The cracks were easy to see, suggesting the cleavage type of cracking associated with torsional shear. This stage of cracking is marked by the number 2 in Fig. 18.

The diagonal cracks had a tendency to become perpendicular to the edge of the bracket as they approached the free edge. This phenomenon is probably due to the absence of torsional shear stress at the free edge. This stage of cracking is marked by the number 3 in Fig. 18. In some cases a crack along the side of the loading plate formed at about the same time that the diagonal cracks would form. These cracks are marked 2' in Fig. 18.

After the cracks reached the free edge at approximately $0.6P_u$ they began to extend down the surface of the face of the bracket at about a 25° angle to the bearing surface. This stage of cracks is marked by the number 4 in Fig. 18. As loads were added the cracks continued to open but propogated rather slowly. The cracks did not reach the level of longitudinal flexural steel in the bottom of the brackets until the load reached about 0.8 or $0.9P_u$. This stage of cracks is marked by the number 5 in the diagram. The longitudinal bar at the top edge of the bracket, which, was used as an anchor bar for flexural steel in the bracket, was believed to have yielded when the loads reached about $0.9P_u$, because the width of the crack appeared

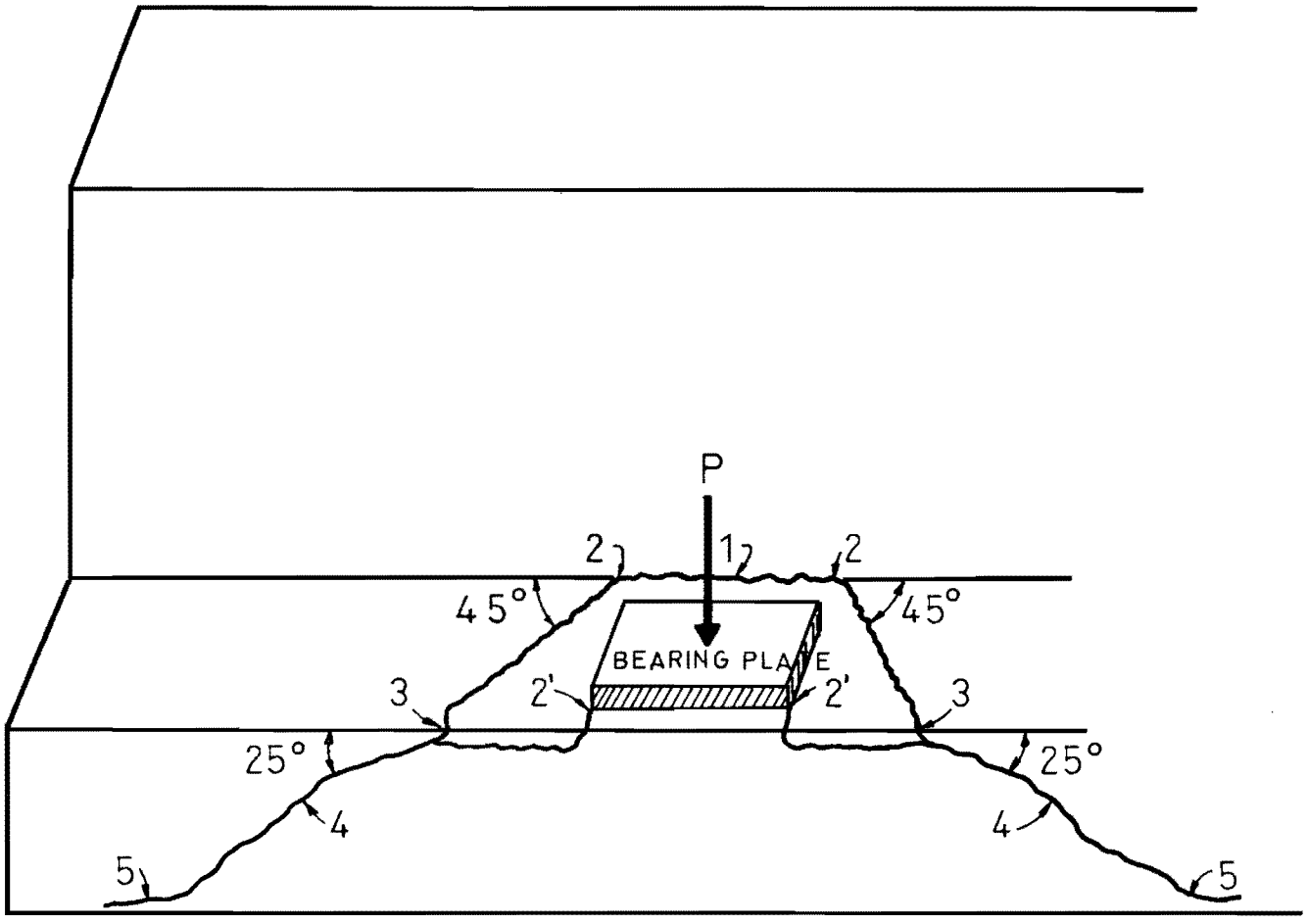

FIG. 18 A TYPICAL "PUNCHING - FLEXURE - TORSION" FAILURE MODE.

to be quite large, in the order of 0.5 in. even on the one-third scale models. As additional load was added the crack opened even larger, and a truncated pyramid of concrete deflected downward. If the stirrups or hangers from the web were relatively light, the truncated portion simply continued to separate from the rest of the beam as load was added. If the stirrups were adequate as hangers to maintain enough load, bracket flexural steel yielded and a secondary compression failure occurred at the bottom of the bracket at the midpoint of the web.

It was impossible to observe the formation of cracks within the region common to both the bracket and the web, unless the load was applied very near the free end of the bracket. Crack patterns at the end of the third model beam are shown in Fig. 19(a). The opposite end of Model Beam 3 is shown in Fig. 19(b). The most prominent cracking appears to begin in the top of the bracket at the web and extend downward across the web. These cracks are caused by tension acting outward due to bracket flexure and downward as the bracket shear loads the hangers. Cracks similar in form undoubtedly occurred at interior regions of beams, although they could not be seen.

Shear Compression Failure in the Web of the T-Beam

Shear compression failure is characterized by the propagation of a diagonal tension crack toward the compression zone of a beam, followed by the eventual crushing-spalling failure of concrete in the compression zone. Figure 20(a) shows a photograph of a specimen after a shear compression failure in the overhanging portion of a beam. The crushing-spalling failure of concrete occurred at the bottom of the specimen. Figure 20(b) shows a photograph of a specimen after shear compression failure in the positive moment region of a beam where the crushing-spalling failure of concrete occurred at the top of the specimen. Crack propagation during the development of a shear compression failure is displayed in Fig. 21. The first visible diagonal crack occurs in the neighborhood of the exterior load, always on the side of the higher external shear, as marked by number 1 in Fig. 21, while the diagonal crack propagates upward into the compression zone of the beam, forming an angle of about 30° to the axis of the beam. The web diagonal

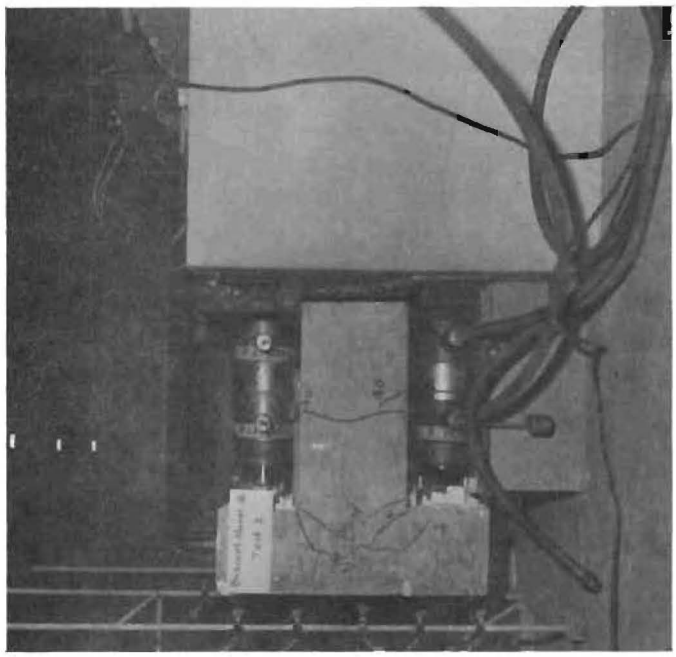

Fig. 19. (a) Failure pattern of BM3 - Test 1.

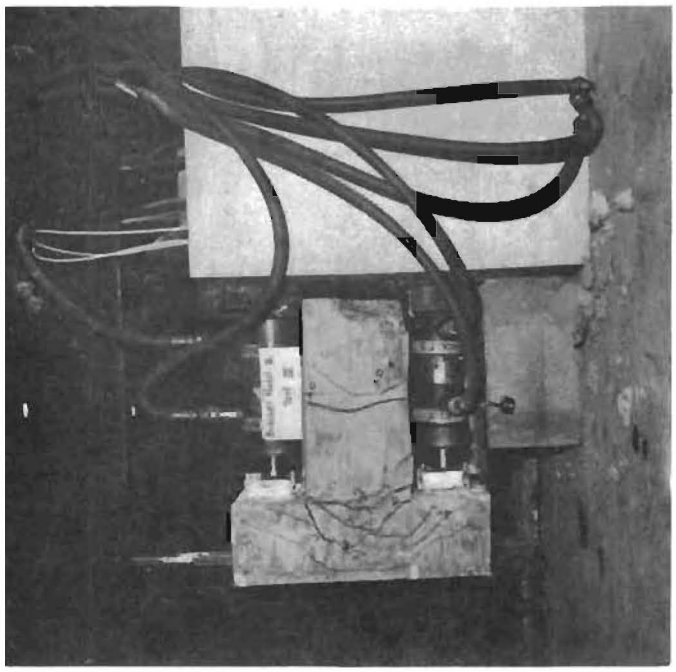

Fig. 19. (b) Failure pattern of BM3 - Test 4.

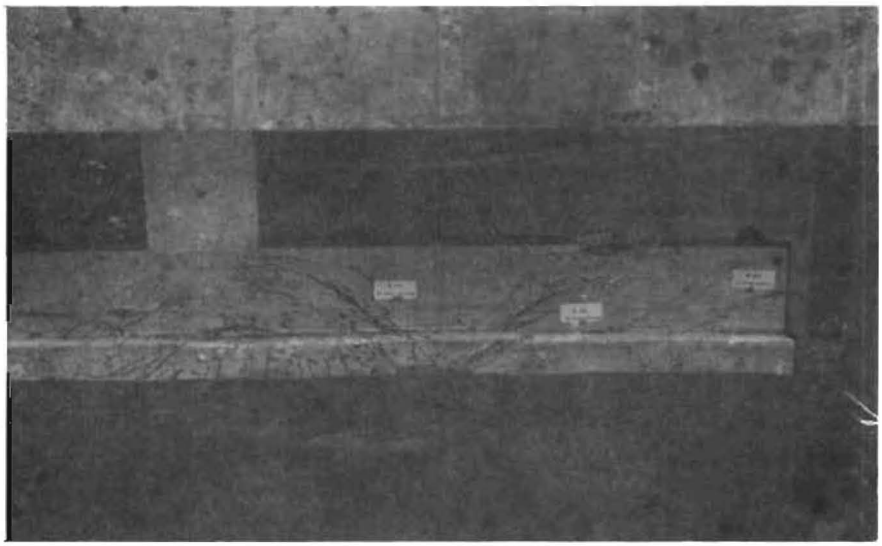

Fig. 20. (a) Shear compression failure at the bottom of a cantilever beam.

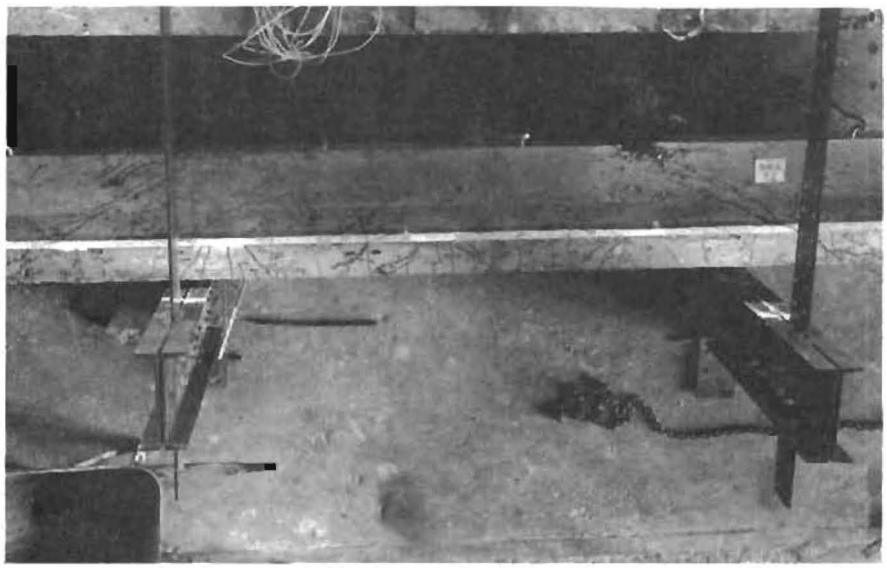

Fig. 20. (b) Shear compression failure at the top of a simply supported beam.

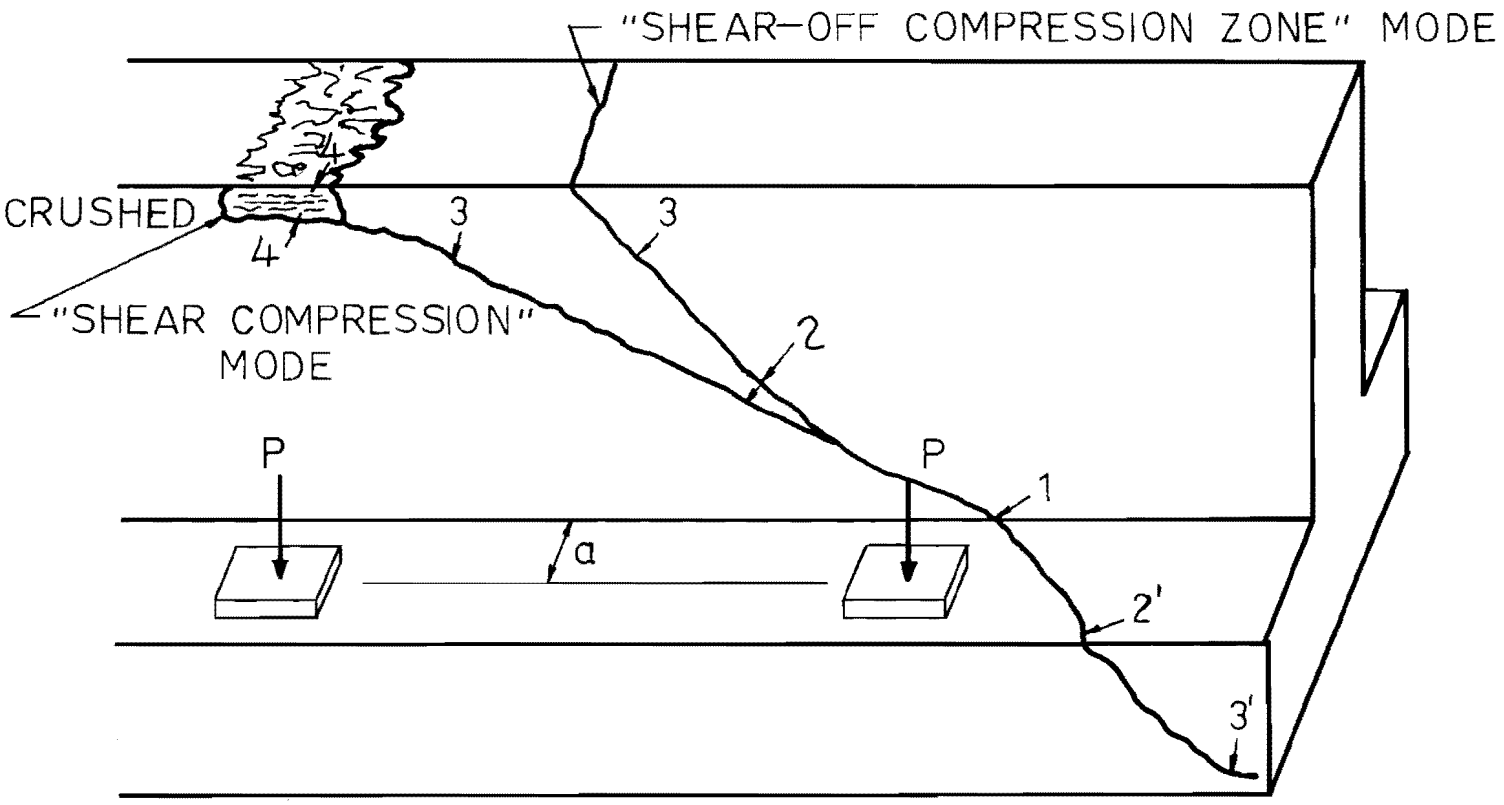

FIG. 21 TYPICAL WEB FAILURE PATTERNS

crack is marked 2 in Fig. 21. A torsional component of shear stress extends the crack in the other direction, marked 2', along the top of the bracket. Considerably higher loads are required before the diagonal crack develops to either point marked 3 in Fig. 21, approximately the level of the compression steel. Rather suddenly another crack propagates on the brackets along the tension steel marked 3' in the diagram. At this stage the crack from 1 to 2' opens to about 1/4 in. of width, even in the one-third scale beams, and the diagonal tension capacity of the bracket concrete generally appears to be exhausted. With further loading the compression zone at 4 crushes, or near the end of the beam anchorage failure of longitudinal steel also might occur.

In some cases the diagonal tension failure did not develop completely into a shear compression failure, but the diagonal line propagated to the compression face before failure took place. Figure 22(a) contains a photograph of Beam Model 2 after test 2, in which a shear failure occurred in the cantilever end of the beam, and Fig. 22(b) shows a photograph of a shear-type failure for test 1 in a positive moment portion of Model Beam 4. Test 1 on Model Beam 4 produced a failure with diagonal cracking in a part of the web subjected to very high compression near the left reaction. The cracking was similar to compressive splitting. The diagonal cracking and subsequent shear failures occurred in beams with smaller ratios of shear span to depth than those for beams that developed shear compression failures. Shear compression failures did not occur in specimens for which the shear span/depth ratio a'/d was smaller than 1.07 in the overhanging region or 0.6 in the simply supported region of a beam. The diagonal tension or shear failure only occurred when the a'/d ratio was small enough that there was more than adequate flexural compression strength in the T-beam concrete to resist whatever moment was developed by the shear acting through the shear span distance a'.

V.

DESIGN CONSIDERATIONS

Bracket Reinforcement

The bracket of an inverted T-beam is actually a deep cantilever shelf continuous longitudinally along the web of the T-beam. The web

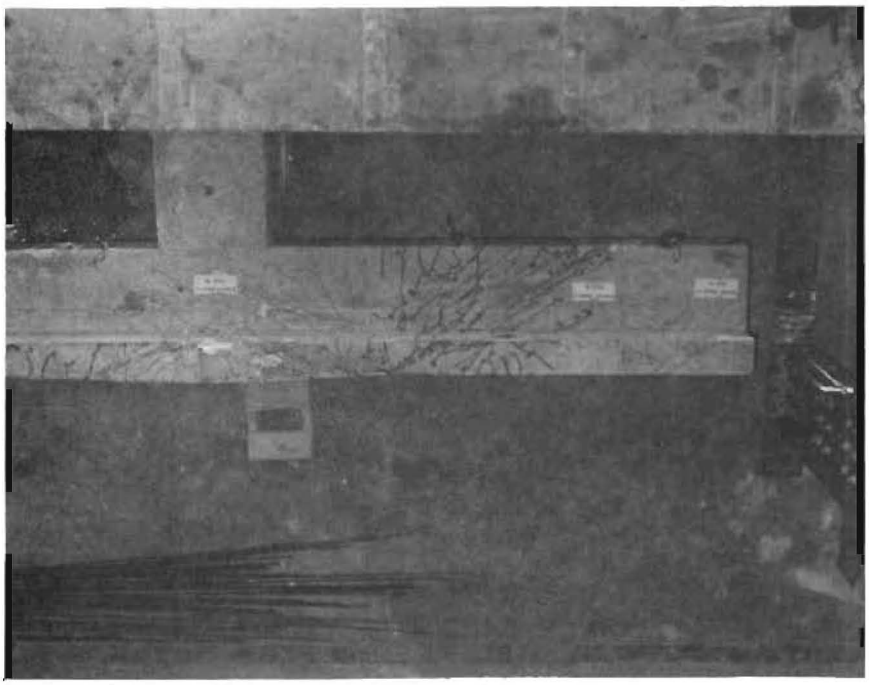

Fig. 22. (a) Cracking at shear failure in negative moment region.

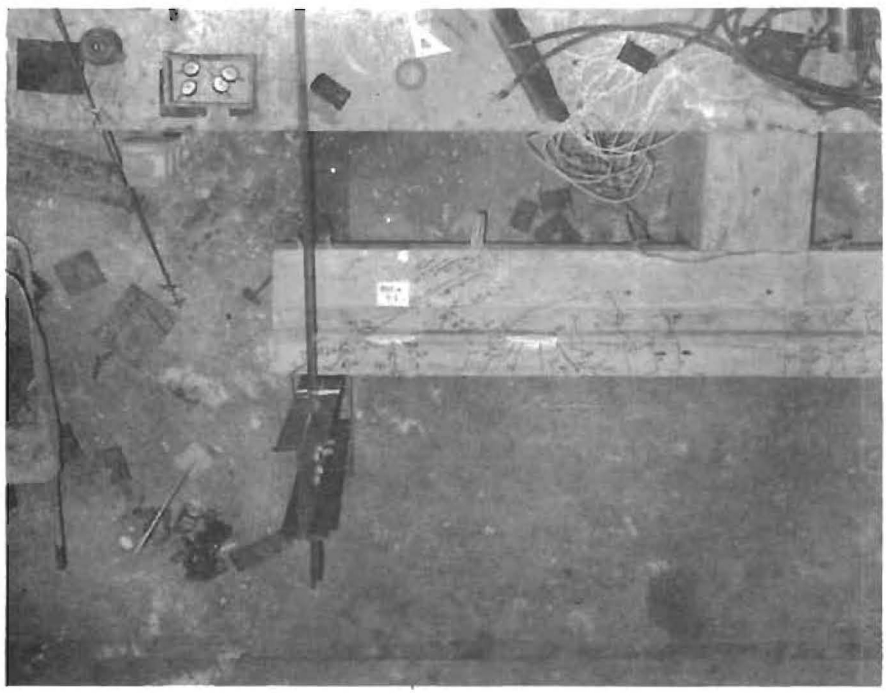

Fig. 22. (b) Cracking at shear failure in positive moment region.

provides support for the bracket in the manner of a fixed edge, but the web obviously is not an absolutely rigid, fixed edge. When the inverted T-beam serves as a bent cap girder, concentrated forces are applied to the bracket at specific locations along the length of the girder, and the design of reinforcement in the bracket must be adequate to sustain bending moments and shears when forces act only at one load point or simultaneously at more than one load point. The equations of statics for cantilever beams are quite simple, and the total moment or the total shear at the fixed edge is easy to determine. However, for deep beams or brackets, the longitudinal distribution of the total moment or the total shear along the fixed edge and vertically through the depth of the bracket, depends upon the elastic properties of the bracket, the description of the area loaded by concentrated forces, and the elastic properties of the supporting fixed edge. Consequently, the analysis of force distribution within the bracket involves a highly indeterminate problem, complicated by the presence of reinforcing bars which do not even resist significant forces until concrete cracks.

Analytical Considerations for Bracket Behavior

The variation of bending moment along the fixed edge of a cantilever plate subjected to a concentrated force P acting at a distance a from a fixed edge results in an expression for the moment m and a shearing force v per unit of plate length given by the following equation:[1]

$$m = -\frac{P \cos^2\alpha}{\pi} \tag{1}$$

$$v = \frac{2P \cos^3\alpha}{\pi r} \tag{2}$$

in which r is the distance between the point of load and a point along the fixed edge; α is the angle between an axis perpendicular to the fixed edge and a line connecting the load point with the reference point along the fixed edge.

The theoretical variations of unit moment and unit shear along the fixed edge are shown by the graphs of Fig. 23. Moment and shear graphs in Fig. 23 were determined for the force P concentrated at one point, and a second set of lines shows the variation of moment and shear if the force P

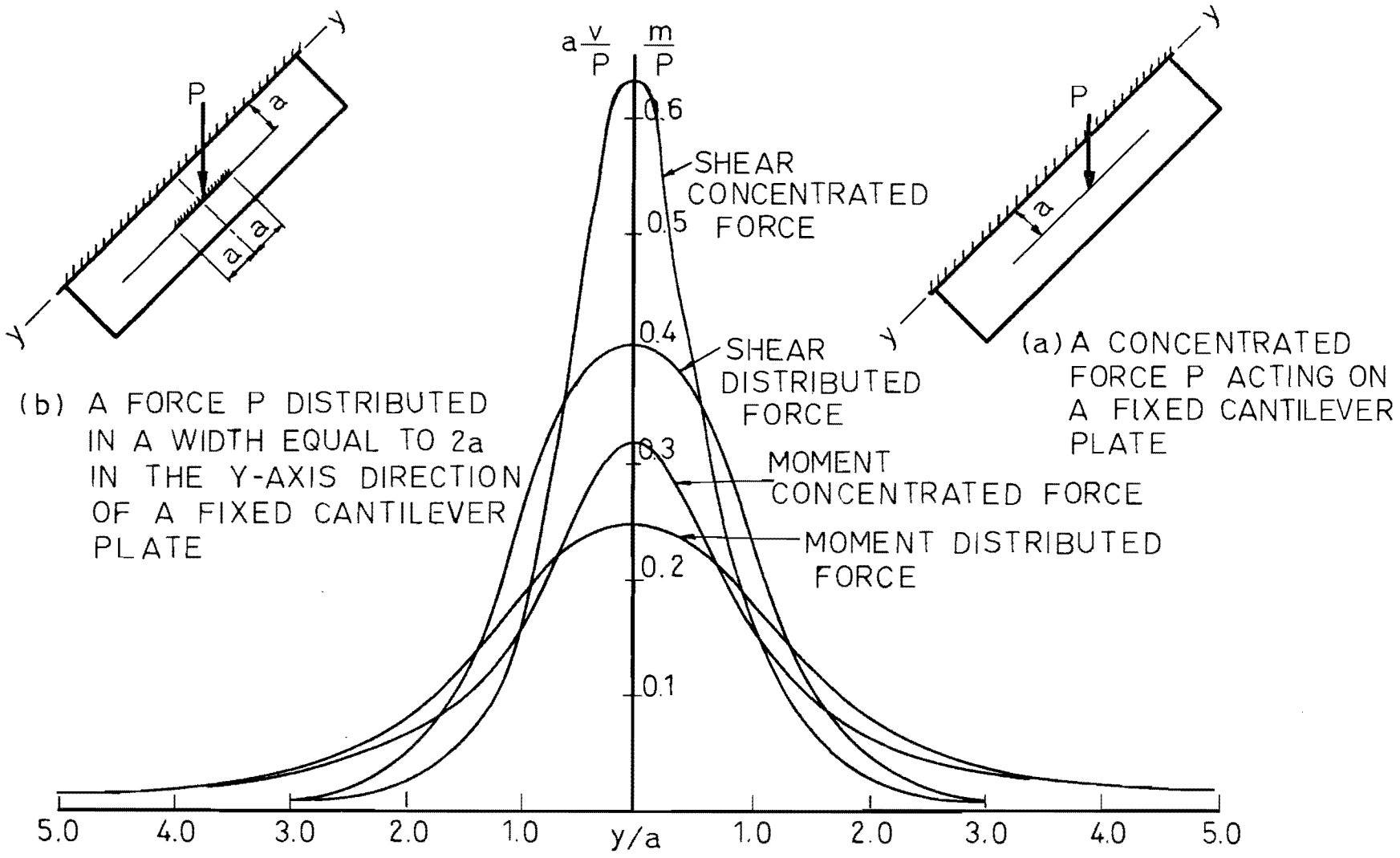

FIG. 23 MOMENT AND SHEAR DISTRIBUTION CURVES ALONG FIXED EDGES OF CANTILEVERED PLATES.

were distributed over some finite length a of the plate. Although the curves of Fig. 23, which show the distribution of shear and moment for a thin plate, are not directly applicable for deep plates, the variation of unit forces along a fixed edge should have some of the same characteristics as those obtained from thin plate theory. Essentially, note that the maximum unit moment and the maximum unit shear at the fixed edge occur directly opposite a point at which the load is applied. Note also that when the unit force is expressed as a ratio of the total force applied, a smaller ratio exists when the load is distributed over some finite length than when the load is concentrated at one point.

Variation of stress through the depth of the bracket at the fixed edge was studied analytically with a finite element model shown in Fig. 24(a). The computed stress along the section marked x-x is shown in Fig. 24(b) together with a straight, dashed line marked Navier's assumption. Navier's analytical assumption, that sections plane before bending remain plane after bending, is not appropriate for deep cantilevers loaded near the fixed edge. In the deep cantilever there is a very high tensile stress at the top of the bracket and a distribution of compression stress over a depth of the member larger than that indicated by linear, first order theory. If a reinforcing bar were visualized at the top of the cantilever, the probable distribution of stress after cracking is likely to be similar to that shown with all tension concentrated at the bar.

The bracket thickness would then be limited to the depth d from the bottom of the bracket to the centroid of bracket flexural steel. The significance of the analytic treatment is the evidence that the probable jd value in a deep cantilever will be smaller than that of an ordinary depth, shallower beam. The finite element analysis suggests that the value kd = 5/8d, and the corresponding value of jd would be d(1 - 5/24) or 0.8d.

After some yielding of bracket flexural steel, the value of jd could be expected to increase. However, in the length of bracket each side of the point of load, bracket steel less highly strained (even though yielded) would be associated with the smaller values of jd. As an average and simple value for data interpretation, jd was taken to be 0.8d for bracket flexure at all levels of load.

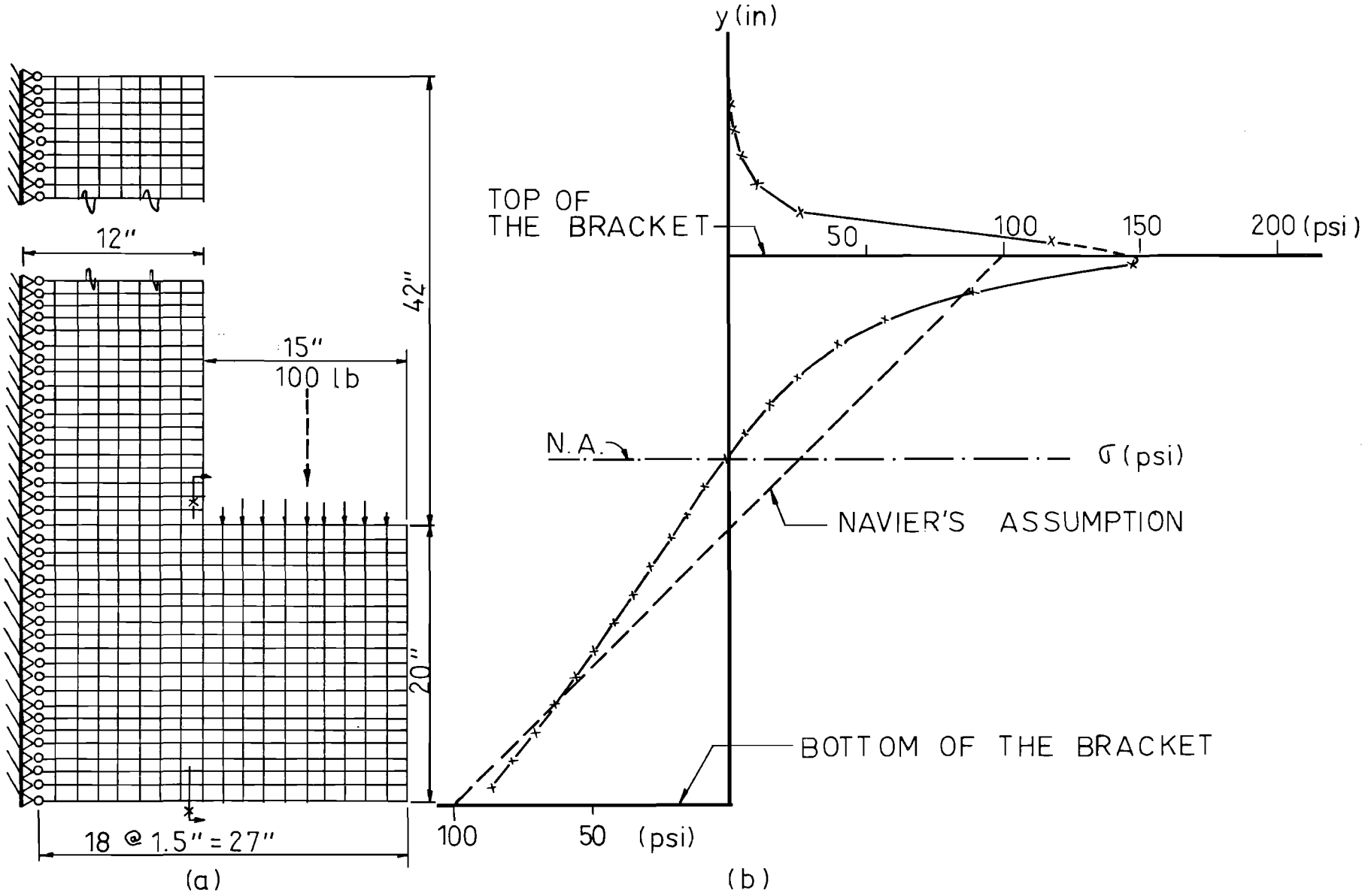

FIG. 24.- FINITE ELEMENT ANALYSIS OF T-BEAM BRACKET FLEXURE.

Measured Longitudinal Distribution of Bracket Moment

The total moment applied to a bracket is the product of applied force times the distance from the force to the base of the bracket, and the total moment is more easily determined than the portion of moment resisted by each reinforcing bar. In order to display measured data in a nondimensional form, useful both for the full-scale specimens and the model specimens for all levels of load, the increment of moment resisted by each cantilever portion was divided by the known total moment on the bracket. Figure 25 contains a representative distribution curve of moment taken from test 3 on Model Beam 4. In Fig. 25 ordinates are ratios between moments at each bar and the total moment on the bracket and abscissae represent distances from the point at which the concentrated force was applied. The distribution curve data for moment at a force P = 15k are shown with circles and the same data for the load P = 52.5k are shown with squares. The circles and squares occurred at each location of a flexural reinforcing bar in the bracket. In a rather typical demonstration of resistance to moment, the distribution is more uniform at the high load after rather extensive cracking in the bracket compelled reinforcement away from the point of loading to share equally in resistance of moment. Simply as a matter of interest for comparison with the data, the elastic analysis distribution curve of moment on a plate cantilevered from a fixed edge and loaded by a force distributed along the same area as that occupied by the bearing plate for the test load, is shown as a dashed line with each set of data. The test data show that cracking and yielding generates a wider distribution of maximum moment.

The distribution curves for moments in test 5 of full-scale Beam 1 (as shown in Fig. 26) show measured distributions wider than those predicted from elastic theory. The same trend is apparent for test 3 of full-scale Beam 1 in Fig. 27. Flexural steel as far from the point of load as two or three times the load moment arm from the face of the web appears capable of developing as much force as the steel directly beneath the point at which load is applied. Figure 27 for the third test on full-scale Beam B1 suggests that bracket flexural steel between the point of loading and the end of the bracket tends to resist a higher proportion of moment than corresponding bars located in the opposite direction from the point of loading.

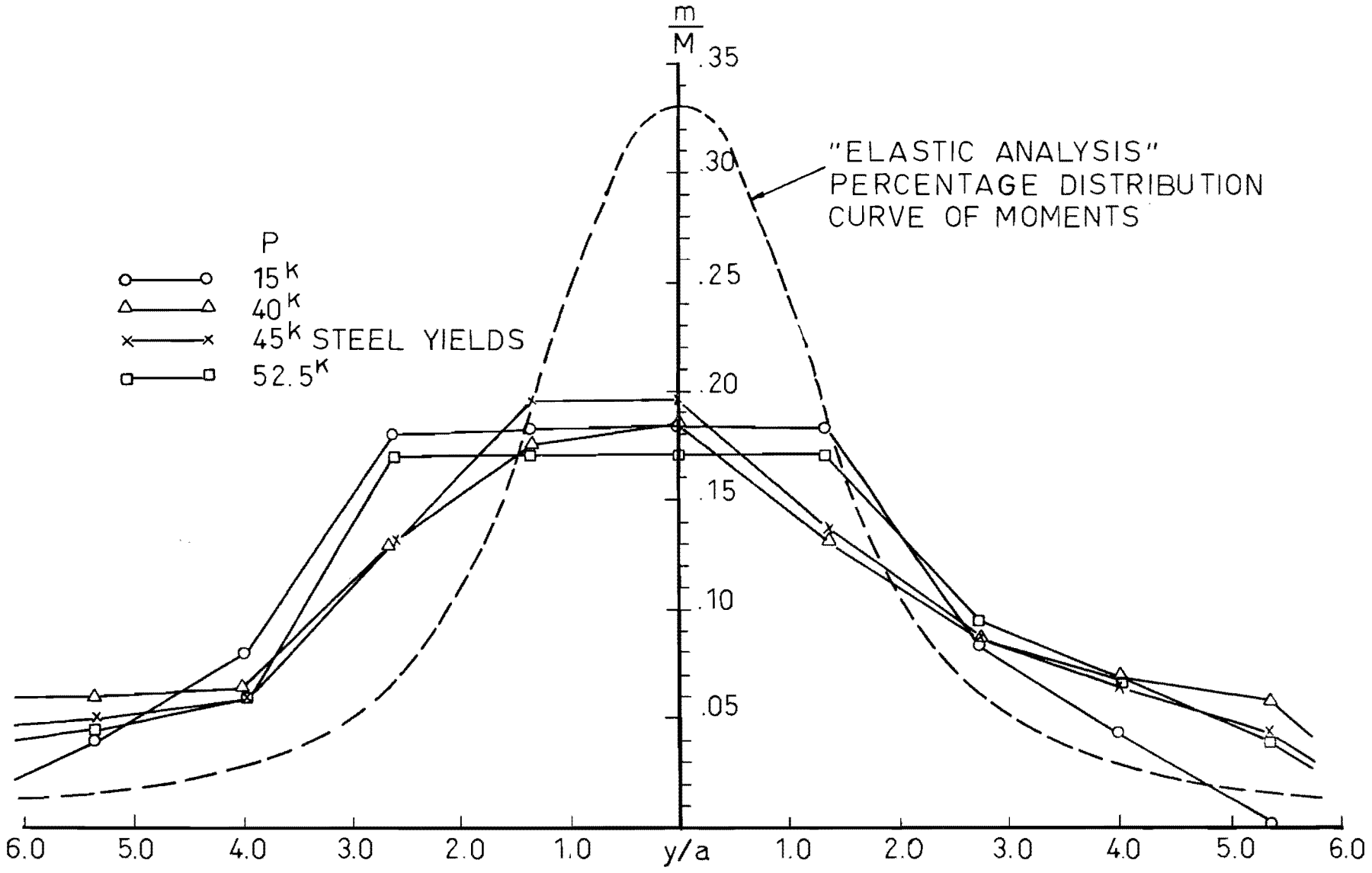

FIG. 25 LONGITUDINAL DISTRIBUTION OF MOMENTS, BM4-T3

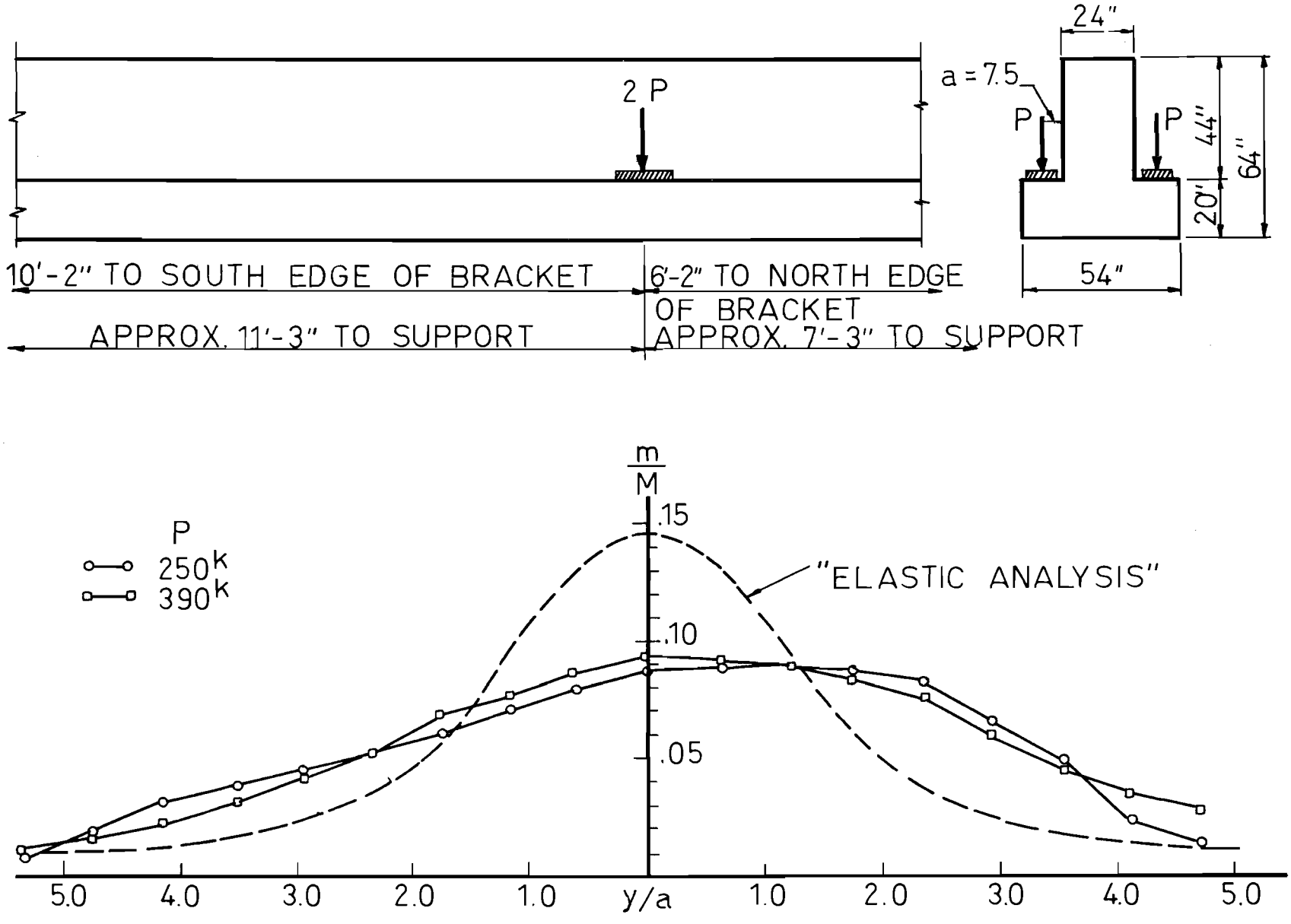

FIG. 26- LONGITUDINAL DISTRIBUTION OF MOMENTS, B1-T5

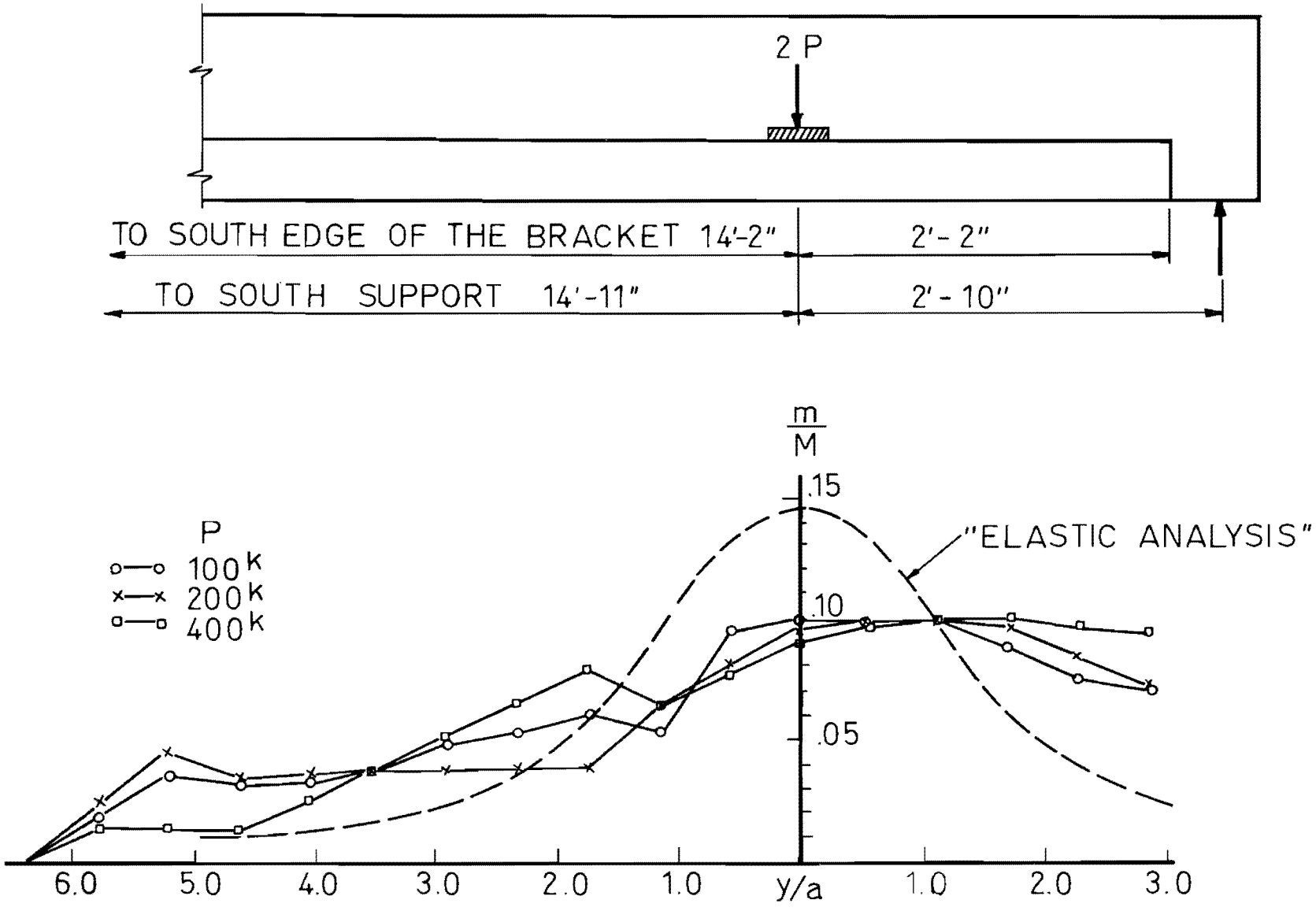

FIG. 27 - LONGITUDINAL DISTRIBUTION OF MOMENTS, B1-T3

A more extreme condition in which the load was applied very near the end of a specimen produced the distribution curve for moments shown in Fig. 28, taken from test 1 on Model Beam 2. The flexural bar at the extreme end of the beam resisted a higher percentage of moment than any of the other bars, and the participation of each bar tended to decrease from the end of the specimen toward the point of support. Strains on these bars indicated that none of the bars had yielded at the time the ultimate load of 29.3k was reached. The distribution curve of moments for load applied near the end of the specimen, shown in Fig. 27, taken for test 1 of full-scale Beam 2 showed the bar toward the end of the specimen resisting a higher percentage of moment than corresponding bars in the opposite direction from the point of load. None of the bars for test 1 on Model Beam 2 developed strains high enough to yield a bar.

Summary of Flexural Behavior of Brackets

When load is applied to the bracket at interior regions of the beam, the centroid of the distribution curves for moment is close to the point at which load is applied but when load is applied near the end of the beam, the centroids of the distribution curves for moment move toward the end of the bracket. Torque must exist in the bracket at the face of the web because of the distance between the centroid of the distribution curve for moments and the centroid of the load. The twist due to such torque helps to explain the development of cracks shown in Fig. 19, which shows the end of Model Beam 3 after test 1. The supplementary shear stresses caused by the twist would add to flexural shear stresses on one side of the point of load, and they would subtract from flexural shear stresses on the other side of the loaded region. Consequently there is no need to superimpose the twisting torsion stresses upon flexural shear stresses based on observed bar stresses or shear friction stresses computed at the interface between the bracket and the face of the web.

The tendency to twist at the end of the bracket appeared to decrease the effectiveness of the flexural steel in the top of the bracket between the load point and the end of the bracket. When the bracket is loaded at some distance from the end, as indicated in Fig. 26, approximately 16 bars

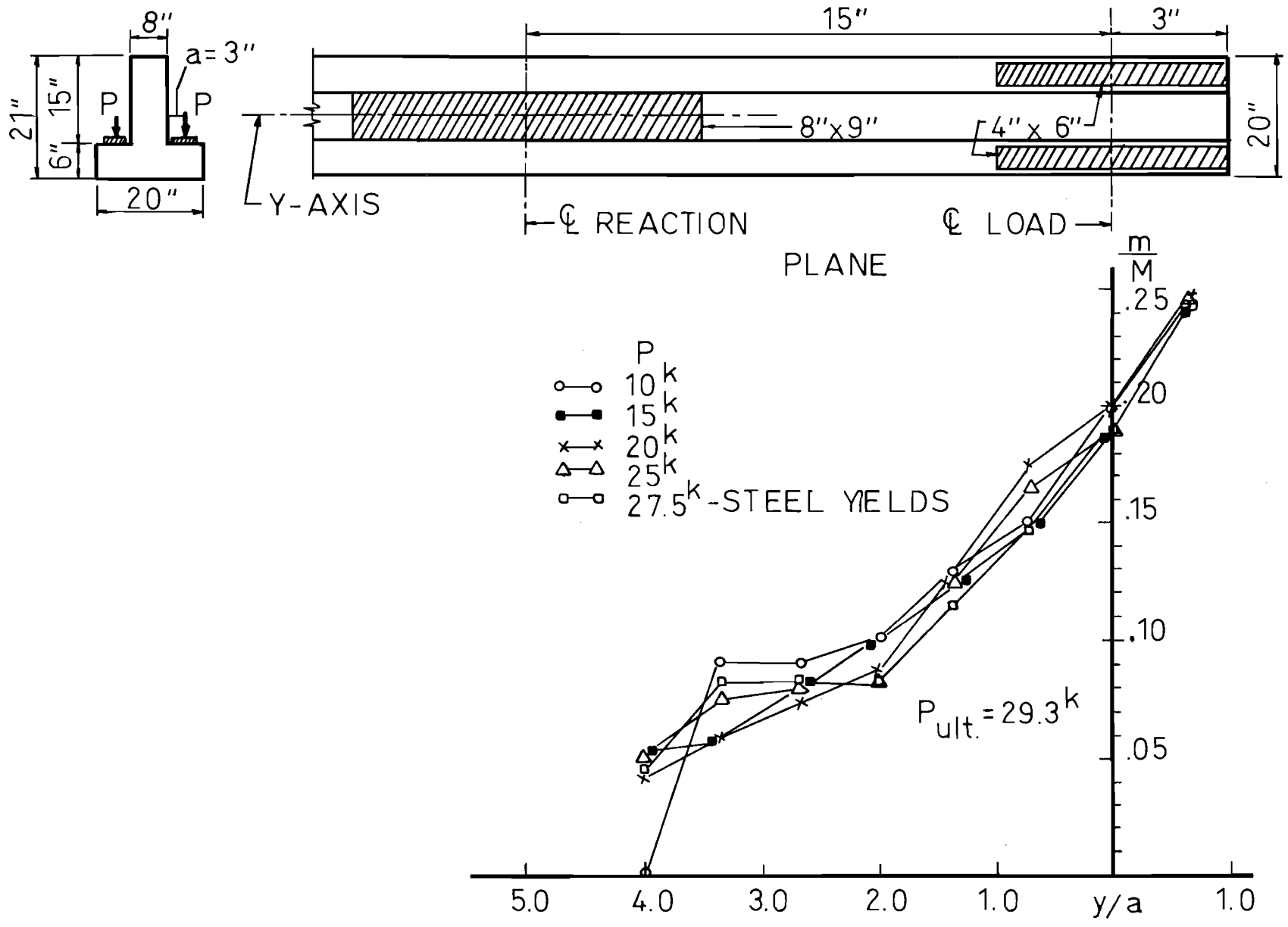

FIG. 28- LONGITUDINAL DISTRIBUTION OF MOMENTS, BM2-T1

shared in carrying substantial flexural stress in the top of the bracket, but in Fig. 28 for which the concentrated load was applied very close to the end of the bracket, only 8 bars carried significant amounts of flexural stress in the top of the bracket. It is doubtful that yield stresses could have been developed in more than 4 or 5 reinforcing bars near the end of the bracket in test 1 of full-scale Beam 2.

Using as an index the distance 'a' from the face of the web to the center of bearings for concentrated load applied to a bracket, for the observations of these tests the width within which flexural reinforcement for brackets must be placed should extend a distance not more than 2.5a each side of the area of loading. When loads are closer than 2.5a to the end of the bracket, the effective width for flexure should be no greater than twice the end distance. The use of 5a plus the width of bearing as the effective width of a bracket for the distribution of flexural steel in the top of a bracket, would have been conservative and safe for the design of the inverted T-beams tested in this series. The use of an effective bracket width smaller than that which might possibly develop also tends to make the effective value of jd (the distance between the center of compression and the center of tension for flexural calculations) smaller than that which would exist if a wider effective section were used in calculations. A 10 percent longitudinal component of live load stringer reactions should be included for the design of flexural steel in the top of the bracket. The rigidity of the bridge deck tends to spread such loads among all stringers, and the approximations used in estimating the effective width for flexure hardly justifies the superposition of tension due to longitudinal force and flexure unless stringers are spaced more closely than 5a plus the width of bearing.

The test measurements and the finite element analysis of the distribution of flexural stress and the web-bracket interface indicate that the characteristic value of jd would be $d - \frac{1}{3} \times \frac{5}{8} d = 0.8d$. Flexural steel should be proportioned for ultimate moments acting on a width no greater than 5a plus the width of bearing, and the value of jd used for flexural steel calculations should be taken as 0.8d. When jd is taken as 0.8d, the compressive capacity of concrete need not be checked.

Shear Strength of Brackets

The flexural capacity of brackets can be considered independently, but some flexural steel A_s can be used as part of shear friction reinforcement. The 1971 ACI Building Code[2] specifies that a bracket with a shear-span to depth ratio a/d less than 0.5 may be designed for shear on the basis of shear friction instead of diagonal tension. Only one load position in the series of tests reported here included a ratio a/d less than 0.5, and in that one test, load position 6 in full-scale Beam 1, a shear friction mode of failure developed. The shear friction mode of failure was not observed in any other test. Shear friction failures can be prevented if there is adequate force normal to the shearing face to maintain resistance to failure in the form of sliding friction in the concrete on the potential shearing face. The normal force can be developed with adequate reinforcement through the shear friction surface. The area of such reinforcement A_{vf} must be adequate to develop a force which when multiplied by μ the coefficient of sliding friction for concrete (taken as 1.4 for concrete cast monolithically) is greater than the shear that is to be maintained across the shear friction face. Thus, in the symbols used for the ACI 1971 Building Code, a formula for the required area A_{vf} of steel to develop shear friction becomes

$$A_{vf} = V_u/\varphi f_y \mu \qquad (3)$$

where φ is a capacity reduction factor taken as 0.85 for shear.

In the one test that developed a shear friction failure, a length of bracket equal to 3.5 shear spans to the point of load (or 3.5a) was sheared off during the test. The elastic analysis curves of Fig. 23 indicate that shears distribute longitudinally over less width than do moments. Test 6 of full-scale Beam 1 involved a load applied within eleven inches of the end of the bracket, or at a distance of only 1.7a from the end of the bracket. A safe rule for design of shear friction steel reinforcement should require that the bars to develop A_{vf} be placed at a distance not more than 2a from the point at which the load is applied. Limits to the effective width of the shear friction face should be taken as not more than a distance 4a

from the area on which load is applied or not more than twice the distance from the point of load to the end of the bracket. Thus, the effective width for shear friction calculations should be taken as 4a plus the width of bearing unless loads are applied closer to the end of the support than 2a. The maximum shear stress suggested by the ACI Code to be permitted on the shear friction sliding face shcuild be no greater than $0.2f'_c$.

If the depth of brackets can be determined on the basis of a maximum shear stress $0.2f'_c$ acting on an area with a depth d and a width of 4a plus w, the width of the bearing pad, the following expression for minimum depth can be obtained:

$$d_{min} = \frac{V_u}{0.85(4a + w)(0.2f'_c)} = \frac{6V_u}{f'_c(4a + w)} \qquad (4)$$

Notice in Eq. 4 that the required depth of brackets varies inversely with the shear span distance 'a'. Of course, if values of 'a' are very large, flexural requirements will control the depth of the bracket instead of shear friction requirements.

Reinforcing bars through the face of the web into the bracket must be adequate to develop enough force to maintain shear friction strength in the concrete. Equation 3 provides a formula for A_{vf}, and Eq. 4 indicates a minimum bracket depth d for shear friction requirements. The necessary bracket depth may be even larger if loads are applied at a distance less than 2a from the end of a bracket.

All of the area of steel A_{vf} need not be placed in the top layer of reinforcement for the bracket. For requirements of shear friction alone perhaps 33 percent of the area A_{vf} should be located at some distance below the flexural steel at the top of the bracket. Flexural steel at the top of the bracket can be distributed over a width 5a + w, whereas the area of steel required for A_{vf} must be located within a width 4a + w. After the selection of a required bracket depth based on shear friction and the corresponding area A_{vf} required, the steel available to resist flexure on the bracket should be checked. In checking the area of flexural steel in the bracket, the centroid of compression force should be assumed at approximately 0.2d above the bottom of the bracket, since the effective value of jd = 0.8d.

The ratio a/d at which flexural steel requirements equal the steel requirements of shear friction can be derived approximately by

setting the flexural steel requirement equal to two-thirds of the shear friction requirement A_{vf}. The following equation can be derived:

$$\frac{4a + w}{5a + w}A_s = \frac{4a + w}{5a + w} \times \frac{M_u}{\phi_f f_y jd} = \frac{2}{3}A_{vf} = \frac{V_u}{\phi_v f_y \mu} \times \frac{2}{3}$$

$$\left(\frac{4a + w}{5a + w}\right)\frac{a}{0.9f_y(0.8d)}V_u = \frac{2}{3} \times \frac{V_u}{0.85f_y 1.4}$$

$$\frac{a}{d} = 0.40\left(\frac{5a + w}{4a + w}\right) \approx \frac{1}{2} \qquad (5)$$

For values of a/d less than 0.5, shear friction requirements would govern the amount of steel through the web of the inverted T-beam at the top of the bracket, and for a/d ratios higher than 0.5, flexural steel requirements would govern the amount of steel at the top of the bracket.

Web Reinforcement--Stirrups

Stirrups are placed in webs of beams in order to transfer shear forces across diagonal cracks that tend to form when the diagonal tension resistance of concrete is less than that required by loads applied to the beams. Forces applied to the top of a beam help concrete to resist diagonal tension stresses due to shear on the beam. When forces are hung from the bottom of a reinforced concrete beam, vertical tension stress is created in the beam above the point at which forces are applied. The vertical tension stress tends to increase the probability of diagonal tension cracking in concrete. Inverted T-beams loaded through brackets at the bottom of the web of the T-beam are thus subject to diagonal tension cracking at loads lower than those which applied at the top of the web of the T-beam would cause diagonal tension cracking.

Analytical studies of principal stresses in rectangular beams have been made as a special topic from the theory of elasticity. A classical demonstration of stress function solutions to rigid body problems includes the description of stresses in a rectangular beam supported at the end and loaded by a force uniformly distributed along the top of the beam.[3] Figure 29 contains a description of the variation in normal stress σ_y through the height of a beam in accordance with the classical theory for top-loaded beams. Howland[4] developed an exact solution used for Fig. 30 for the

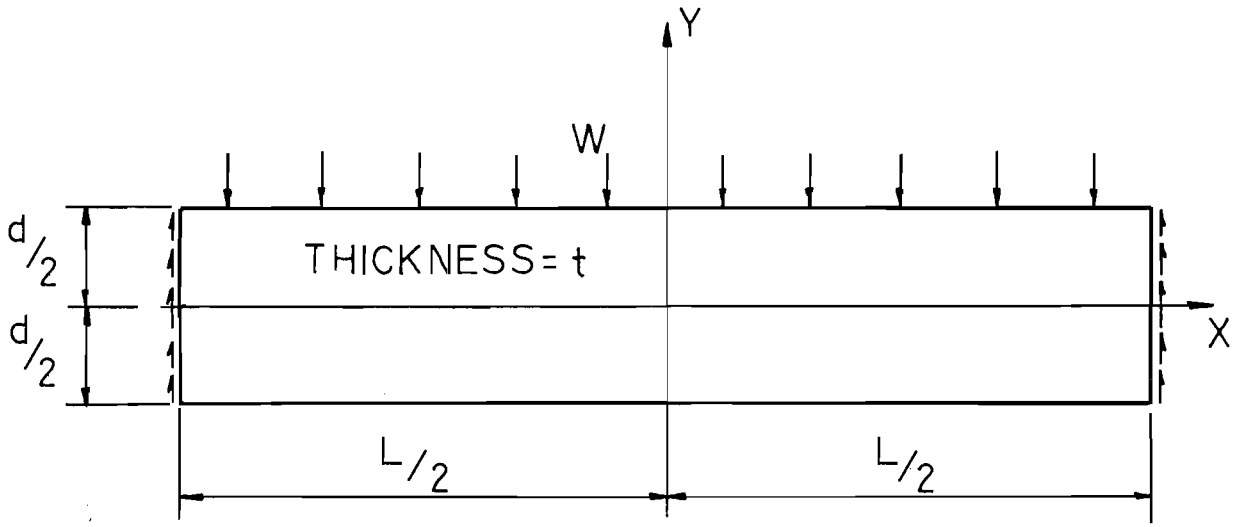

(a) UNIFORMLY LOADED RECTANGULAR BEAM.

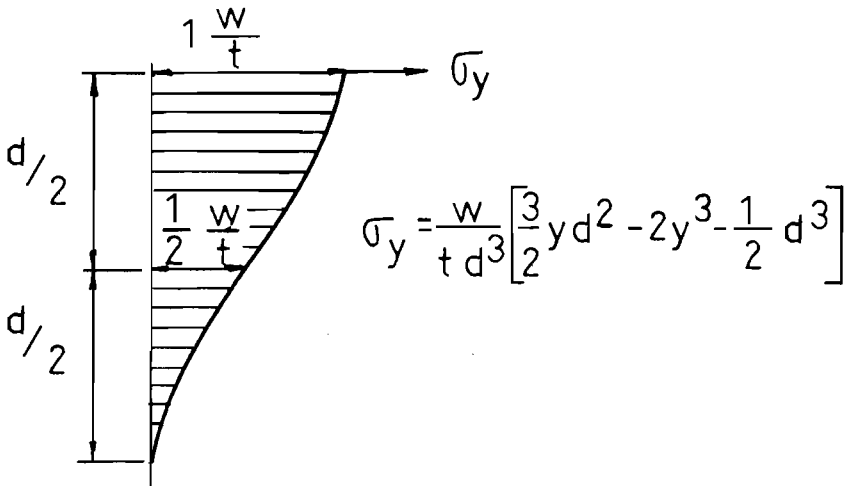

(b) COMPRESSIVE STRESS VARIATION WITH DEPTH.

FIG. 29-CLASSICAL THEORY-STRESSES IN TOP-LOADED BEAMS.

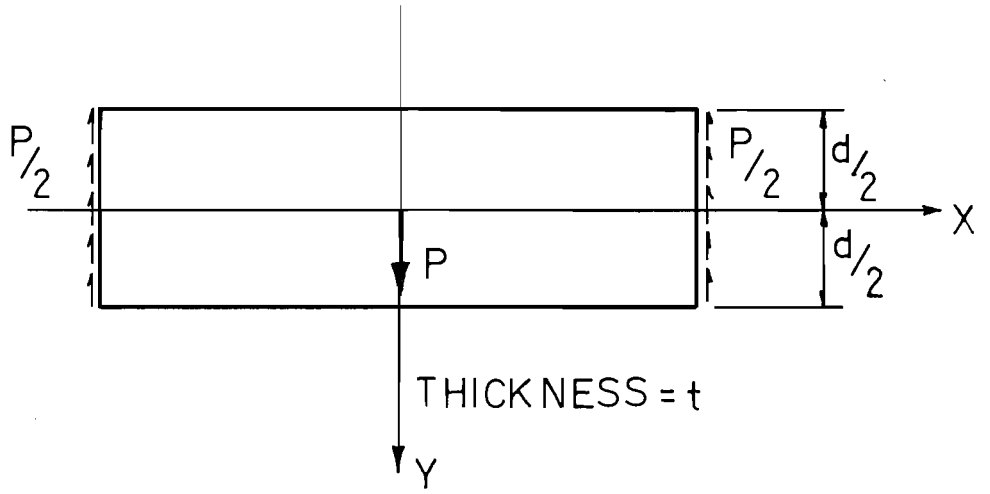

(a) CENTRALLY LOADED PLATE

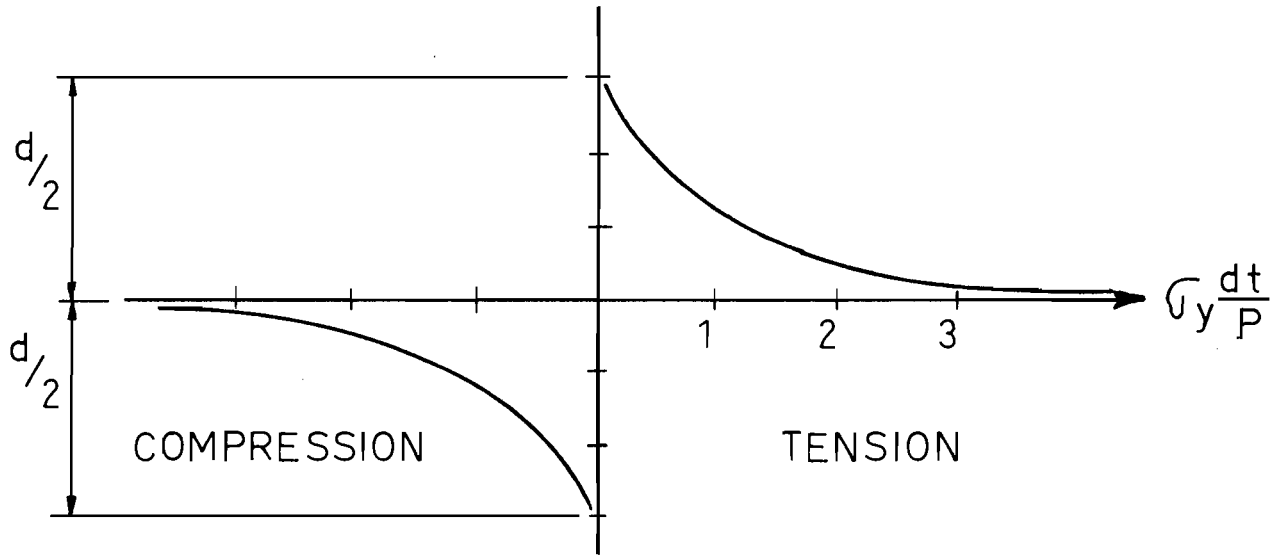

(b) COMPRESSIVE STRESS VARIATION WITH DEPTH

FIG. 30 - CLASSICAL THEORY - STRESSES IN CENTRALLY LOADED PLATE.

problem involving a concentrated load applied at the midheight of a beam. Howland stated that the local effect of a force acting at the center of the height of a beam was insignificant beyond a longitudinal distance approximately 1.5 times the depth of the beam away from the point of load application.

Leonhardt[5] tested rectangular and T-beams with loads acting as side shears rather than compression applied to the top of the beams, and he suggested that the stirrup reinforcement must be so designed that it could carry about 80 percent of the locally applied vertical shears. His shear load was applied through short transverse beams framed perpendicularly into the test beams. On the basis of similar tests performed by Rüsch[6] a suggestion was made that stirrup reinforcement should be designed as hangers to support the full local vertical force, instead of only 80 percent as recommended by Leonhardt. Rüsch reasoned that stirrups designed for the full vertical force would be less likely to undergo large elongation prior to failure. Earlier tests conducted by Ferguson[7] clearly showed that beams could sustain less load when applied on the lower half of the beam as when applied as forces on top of the beams. Although Ferguson did not suggest a specific value for designing stirrups as hangers, he warned that if load were brought in as a shear below middepth, ultimate shear strength was reduced and stirrups were essential for such cases. On the basis of the inverted T-beam tests reported here, the action of stirrups as hangers to transfer loads on the bracket from the lower part of the web to the upper part of the web was rather clearly demonstrated.

Stirrups as Hangers in Inverted T-Beams

Four tests on model beams included in this project failed in a mode that strongly suggested the failure of stirrups acting as hangers in delivering the bracket loads to the upper parts of the inverted T-beam web. The second and third load cases for Model Beam 3 involved the application of loads between simple supports such that the bracket itself was in longitudinal tension, and the loads truly were applied as shears at the lower region of the web of the beam. The longitudinal distribution of hanger force for load position 2 is shown in Fig. 31, and the distribution of force on the

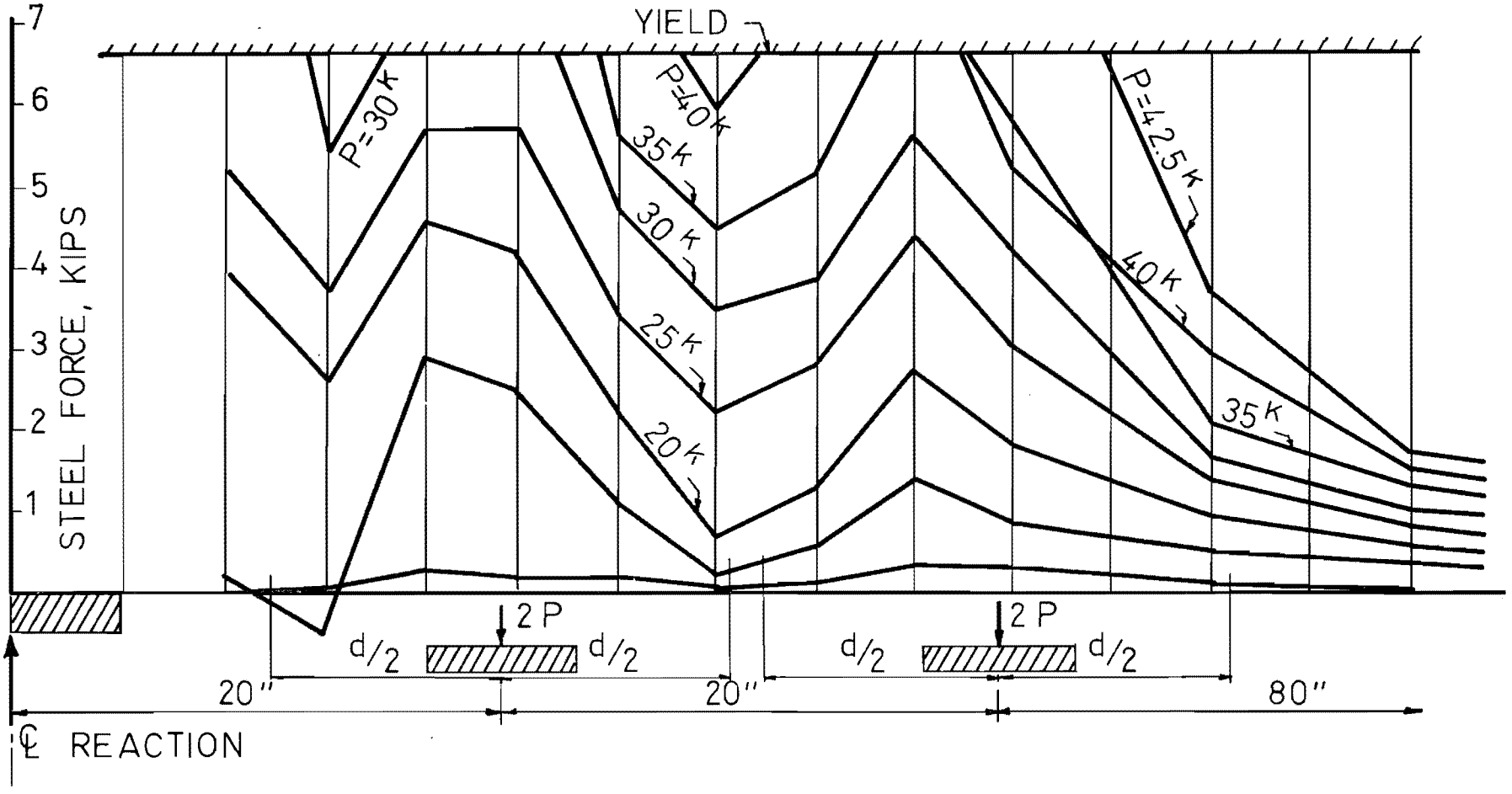

FIG. 31 HANGER FORCE DISTRIBUTION OF BM3-T2

stirrups for load position 3 is shown in Fig. 32. In each figure the load level for each curve is written along the curve. Stirrup forces were obtained from strain gages attached to the stirrup. In Figs. 31 and 32, yield force in the stirrup is indicated by the cross-hatched line at the top of each figure. The figures indicate that all stirrups within a distance of half the effective depth of the beam away from the point of load reached yield strain before failure took place at the highest load level indicated. They show also that the stirrups in the higher shear region of each beam reached yield levels before comparable stirrups on the opposite side of the load point in a region of lower shear on the web reached yield levels. Some additive effect between hanger tension and tension due to web shear is apparent, but the distribution of stress after some yield nullifies such additive effects as a source of failure.

The failure of stirrups acting as hangers in cantilever portions of Model Beam 3 also occurred for load position 1 and load position 4. The longitudinal distribution of stirrup force, measured for load position 1, is shown in Fig. 33, and for load position 4 is shown in Fig. 34. Again, the hangers within a distance equal to half the depth of the web appeared to reach yield loads before the failure of the specimen. Except at the very end of each specimen, the stirrups in regions of higher shear tended to reach yield loads and develop forces higher than those in regions of low shear. Again, for hangers in cantilever regions, the redistribution of stirrup and hanger tension (after some hangers yielded) tended to compensate for any additive effect between tension due to web shear and tension due to hanger force.

For Model Beam 3, the tensile strength of stirrups acting as hangers within a distance of d/2 from the interior points of loading was 53k when stirrups were 6 in. apart in load position 3, and 79k when stirrups were 4 in. apart in load position 2. A force of 70k was resisted in load position 3 before failure, and 80k were supported before the failure of load position 2.

In the cantilever part of Model Beam 3 (Fig. 34) the three stirrups nearest the end should have supported an end force computed to be 40k, and failure occurred at 41.5k. At the other end of the beam, Fig. 33 indicates that four stirrups yielded. One of the stirrups was more than d/2 from the

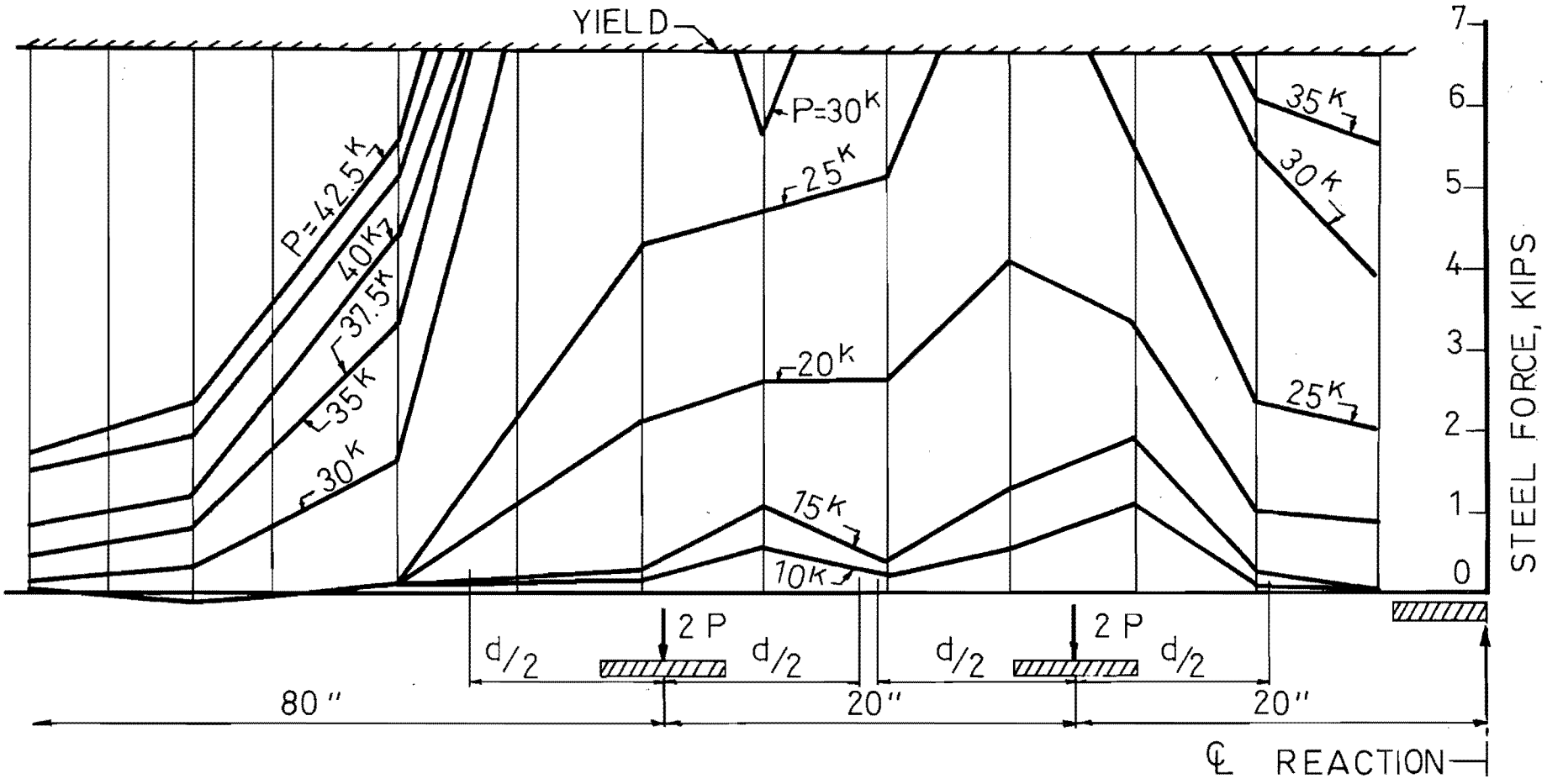

FIG. 32- HANGER FORCE DISTRIBUTION OF BM3-T3

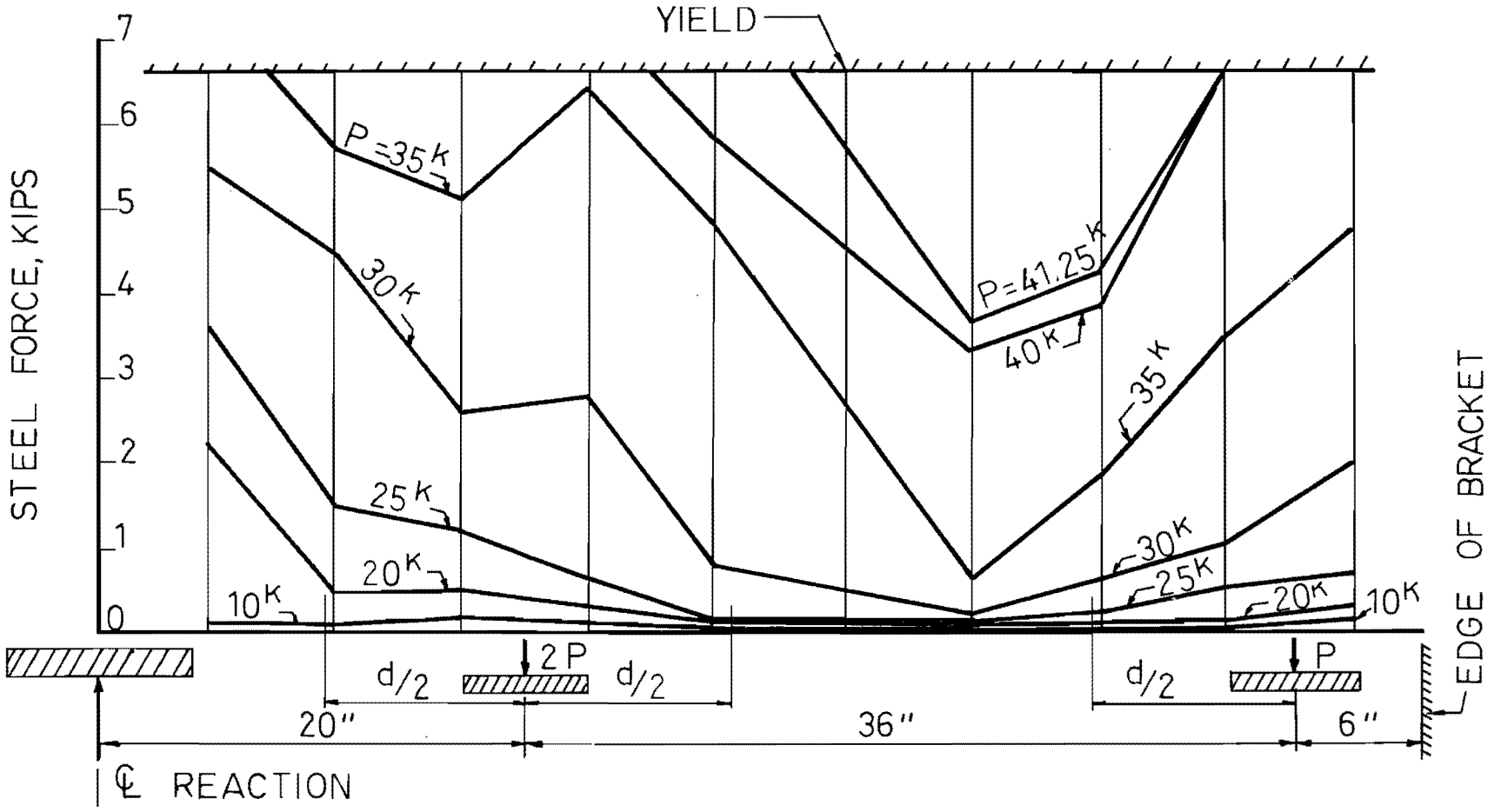

FIG. 33 HANGER FORCE DISTRIBUTION OF BM3-T1

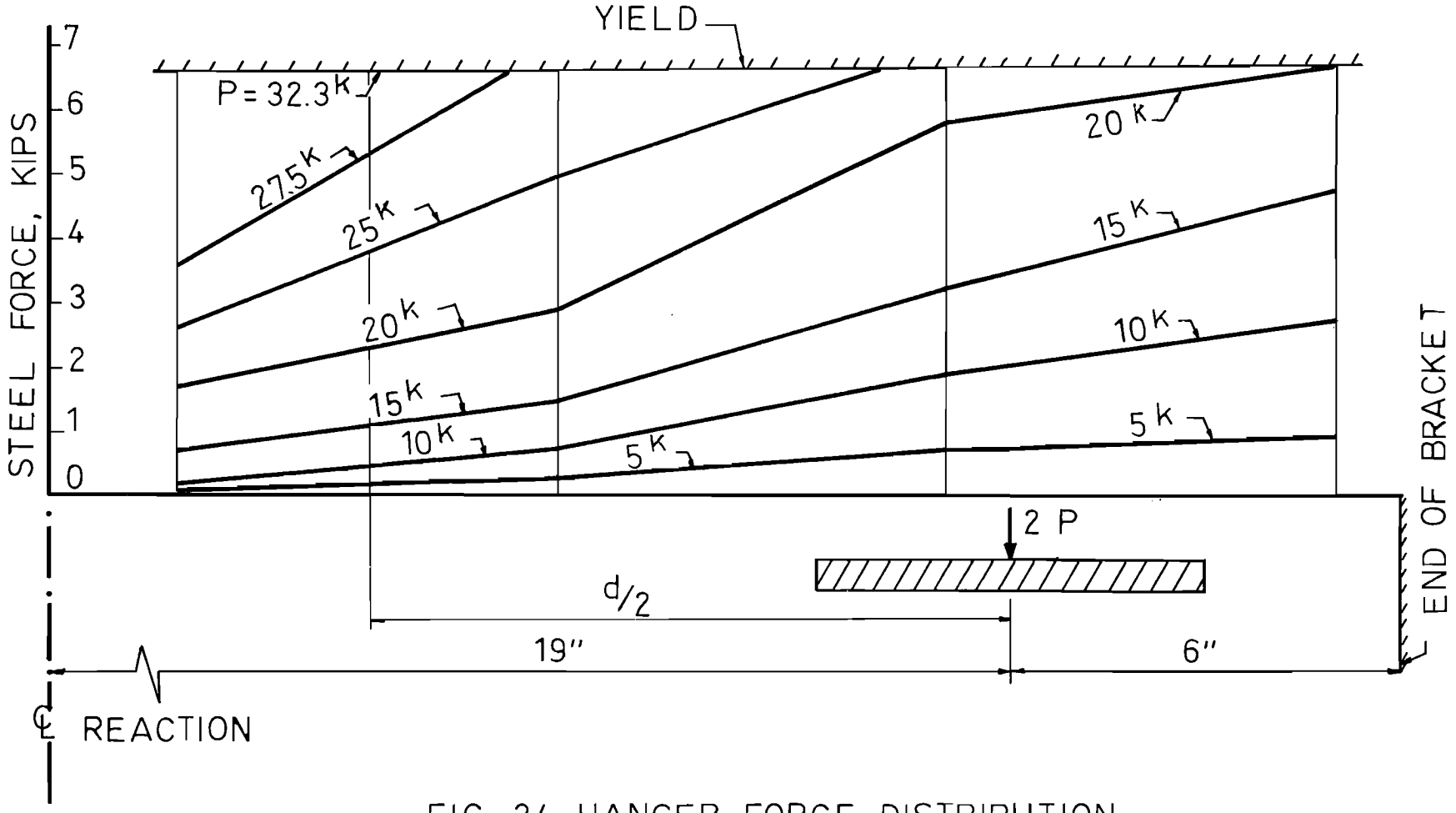

FIG. 34 - HANGER FORCE DISTRIBUTION
OF BM3 - T4

point of loading. The tension capacity of the four stirrups was 53k, and the failure load reached 65k.

For the few cases in which stirrup failure as hangers occurred, all hangers within a distance d/2 from the point of load yielded. In two cases it was possible to apply substantially more load than the tensile capacity of stirrups within a distance d/2 from the point of load, but in the other two cases, failure occurred almost precisely at the same load as the capacity of stirrups within the distance d/2 from the point of load. Therefore, it would appear valid to require stirrups adequate to act as hangers within a total length of d centered about the loaded bearing regions. Hanger capacity can be evaluated simply as the product of stirrup area and the yield stress of the stirrup.

Stirrups as Diagonal Tension Reinforcement

Diagonal tension failures with hanger and shear compression mode complications occurred in at least six of the tests performed on the model beams. In all specimens (as in most bent cap bridge girders) there was a substantial amount of both tension and compression flexural reinforcement available to promote ductility in critical shear regions. Flexural and diagonal cracks usually developed to as much as 1/4 in. width in the one-third scale models prior to failure. The large cracking indicated that forces were being redistributed from highly strained regions to regions with reserve capacity.

Shear strength for the eight tests that produced apparent shear failures was evaluated according to ACI Code provisions with a capacity reduction factor φ taken as unity. Results from the evaluation are displayed in Fig. 35, where values determined from ACI Code formulas are given as abscissae and test values are shown as ordinates. If the test values were the same as computed capacities in accordance with the ACI Code, data points would appear along the heavy black line of equal ordinate and abscissa values. The square data points are based on the simple formula for ultimate shear stress.

$$v_u = 2\sqrt{f'_c} + \frac{A_v f_y}{b's} \qquad (6)$$

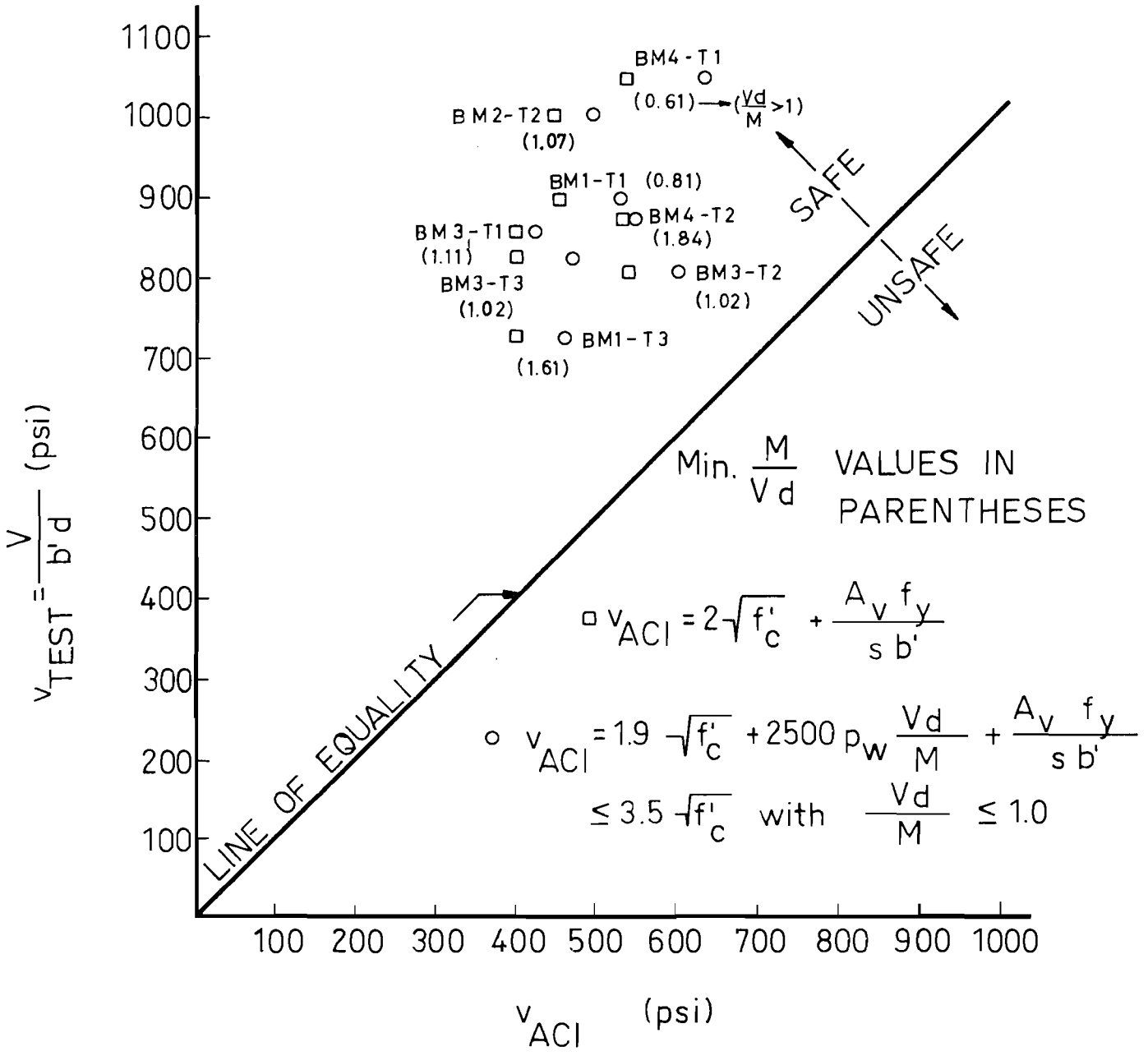

FIG. 35 - SHEAR STRENGTH COMPARED WITH ACI CODE VALUES.

Circled data in Fig. 35 are based on the more complex formula that recognizes shear span and longitudinal reinforcement:

$$v_u = 1.9\sqrt{f'_c} + 2500\, p_w \frac{Vd}{M} + \frac{A_v f_y}{b's} \qquad (7)$$

In Eqs. 6 and 7

v_u = ultimate shear stress in psi
f'_c = compressive strength of standard cylinders in psi
A_v = area of a stirrup cross section in square inches
f_y = yield strength of stirrup steel in psi
b' = width of beam web in inches
s = longitudinal spacing of stirrups in inches
p_w = ratio between longitudinal steel area and b'd
d = depth of beam in inches
V = shear force in pounds
M = moment force in in.-lbs.

Even though the ACI Building Code equations that limit shear stress are expressed in terms of ultimate strength v_u, the equations were intended to prevent large cracking, not necessarily to indicate failure strength. It is apparent from Fig. 35 that stress values determined in accordance with the ACI Building Code are considerably lower than those developed by inverted T-beams tested in this series. It was felt by the investigators that the concrete in the T-beam flanges (or brackets) contributed to the available shear capacity of the beams.

A second comparison of computed ultimate shear stress is displayed in Fig. 36, which shows test values of shear stress computed on the basis of all concrete area above the centroid of longitudinal tension steel rather than the restricted area b'd. Sketches of Fig. 36 demonstrate the shear stress areas used in the figure. Again, all values computed in accordance with stress values from the ACI Code cracking limits are smaller than those determined from tests, but the differences are considerably less than those observed in Fig. 35.

$$\square\ v_{ACI} = 2\sqrt{f'_c} + \frac{A_v f_y}{s\,b'}$$

$$\circ\ v_{ACI} = 1.9\sqrt{f'_c} + 2500\frac{P_w V d}{M} + \frac{A_v f_y}{s\,b'} \leq 3.5\sqrt{f'_c}$$

$$\text{with } \frac{V\,d}{M} \leq 1.0$$

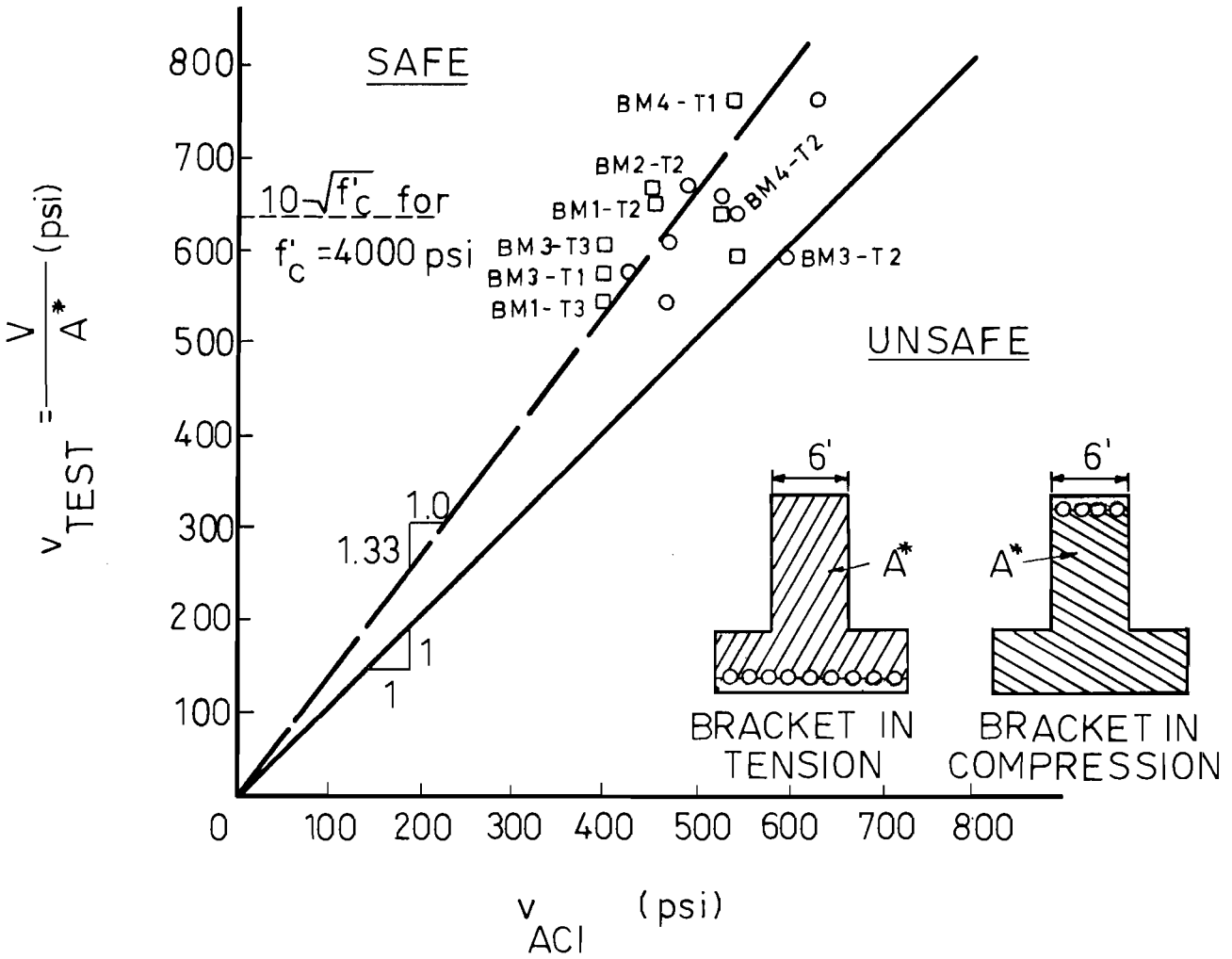

A* — CONCRETE AREA ABOVE THE CENTROID OF LONGITUDINAL REINFORCING BARS.

FIG. 36 - SHEAR STRENGTH COMPARED WITH MODIFIED VALUES OF ACI CODE.

On the basis of the test series reported here, two significant conclusions can be reported.

(1) Stirrups in inverted T-beams can be proportioned for web shear without any hanger stress superimposed on the girder shear stress if ultimate strength limits of the ACI Building Code are observed.

(2) All of the concrete above the centroid of longitudinal tension steel can be considered effective in resisting shear stress in inverted T-beams of the proportions tested and reported.

VI.

CONCLUSIONS

The behavior of reinforced concrete beams with an inverted T cross section has been observed in six test specimens. Each specimen was subjected to several different patterns of load applied to the bracket formed by the arms of the inverted T cross section. Initially, reinforcement was detailed in the same way as that specified for some Texas Highway Department bent cap girders. Subsequently, beams with alternate patterns of reinforcement were constructed and tested. Two specimens were constructed with a cross section the same size as that of the bent cap girders specified by the Texas Highway Department, and four specimens were constructed to one-third the scale of actual highway bridge structures. The full-scale specimens were used primarily to study the reinforcement used in the bracket of the inverted T-beams. One-third scale specimens were useful both for studies of bracket reinforcement and for web shear in the stem of the inverted T cross section.

With one exception, all specimens with dimensions and reinforcement details in accordance with those specified by the Texas Highway Department resisted loads near 400k at any one bearing without failure. The one exception involved a specimen loaded near the longitudinal end of the bracket with forces of 380k applied to each bracket. The most significant conclusions derived from tests of full-scale specimens include:

(1) Brackets reinforced with horizontal bars for flexure and with supplementary horizontal reinforcement parallel to flexural steel approximately at the third point of bracket depth (Fig. 37(a)), performed as well as brackets that were reinforced with a diagonal bar extending from the lower exterior edge of the bracket diagonally upward toward the center of the T-beam stem (Fig. 37(b)). Originally it was thought that the diagonal bar would be important as bracket shear reinforcement at the face of the T-beam stem. Locating and tying the diagonal bar in the form is a cumbersome process, and the more easily constructed horizontal bars appeared to perform equally as well as the diagonal bars.

(2) Stirrups in the stem of the T-beam act as hangers to deliver bracket loads into the upper region of the T-beam stem. In order to serve as hangers the stirrups must be able to develop by bond the tension force each must carry, unless the stirrup is bent across the bottom of the T-beam stem. Brackets generally are not deep enough to develop enough anchorage in hangers. Therefore, stirrups considered to act as hangers should be closed across the bottom of the T-beam, as shown in Fig. 37(c).

(3) The practice of welding bracket flexural steel to an anchor bar parallel to the longitudinal axis of the T-beam appeared to provide adequate anchorage to develop the yield strength of the flexural steel in the top of the bracket.

The following conclusions involving bracket reinforcement were determined from observations both of full-scale specimens and one-third scale specimens:

(1) The width of bracket that can be considered effective in flexure caused by a concentrated load should be no greater than the width of bearing plus five multiples of the distance "a" between the face of the stem of the T-beam and the center of the bearing (see Fig. 38). If the distance c between the edge of a bearing and the longitudinal end of a bracket is less than 2.5a, the effective width of bracket for flexure should be taken as 2c, as sketched in Fig. 38(b). The

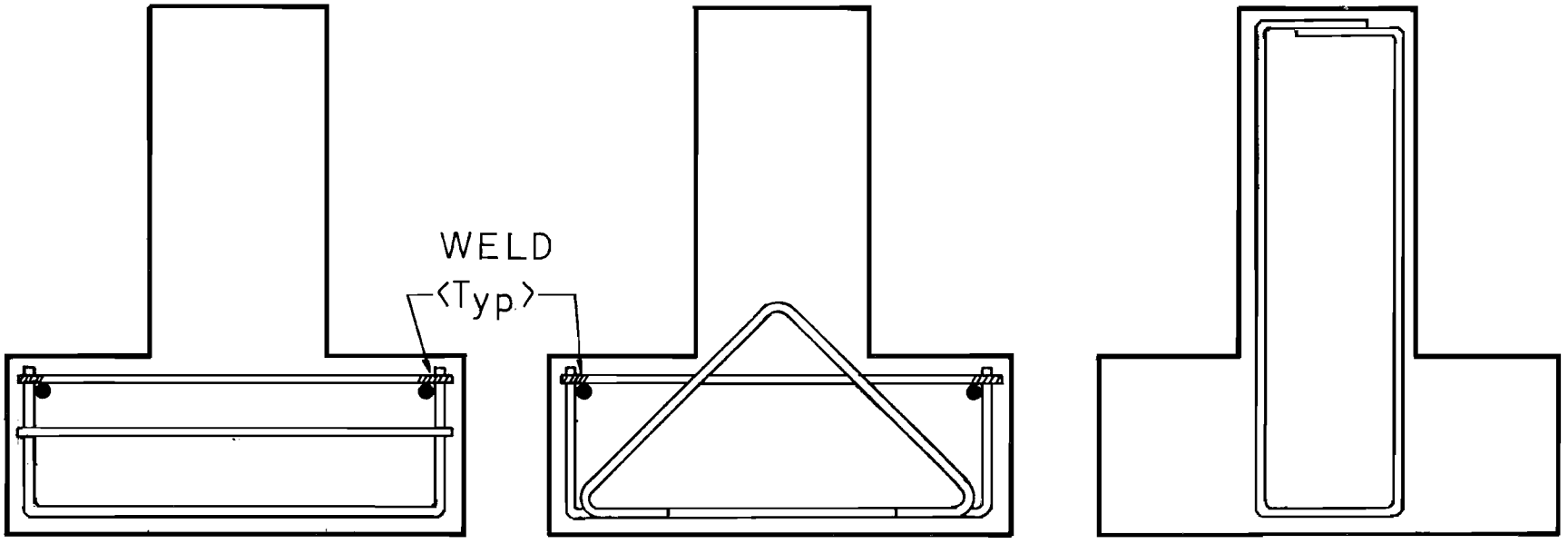

(a) HORIZONTAL BARS (PREFERRED)

(b) DIAGONAL BAR (NOT PREFERRED)

(c) HANGERS MUST BE CLOSED ACROSS BOTTOM

FIG. 37 - BRACKET REINFORCEMENT.

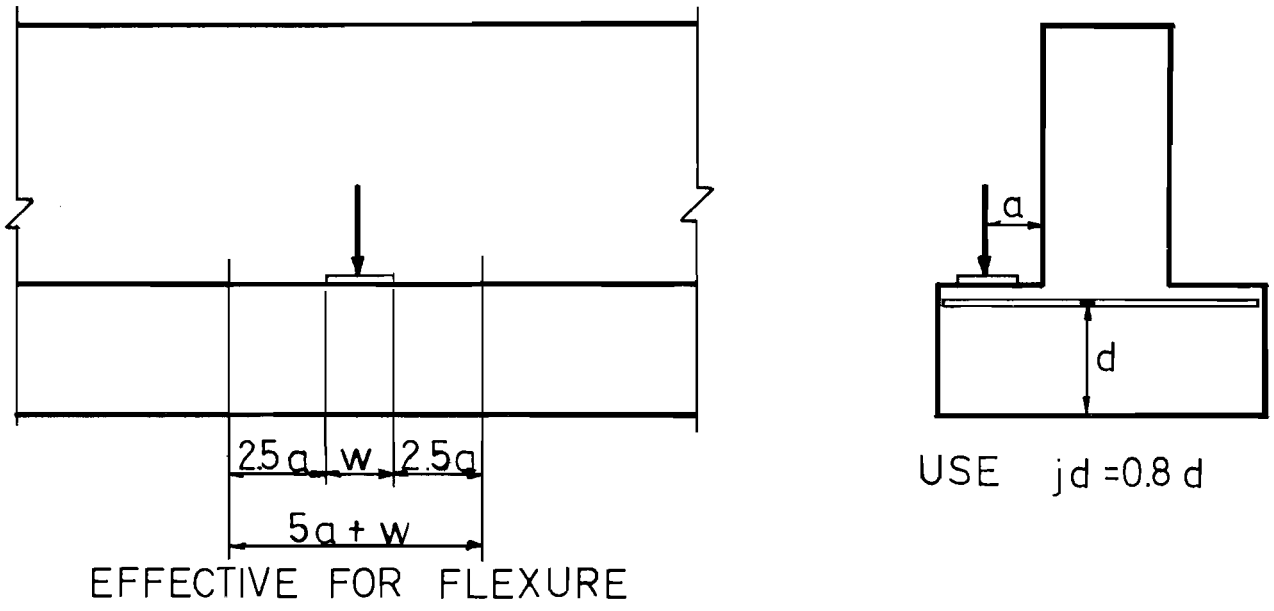

EFFECTIVE FOR FLEXURE

(a) INTERIOR PORTION OF BEAM.

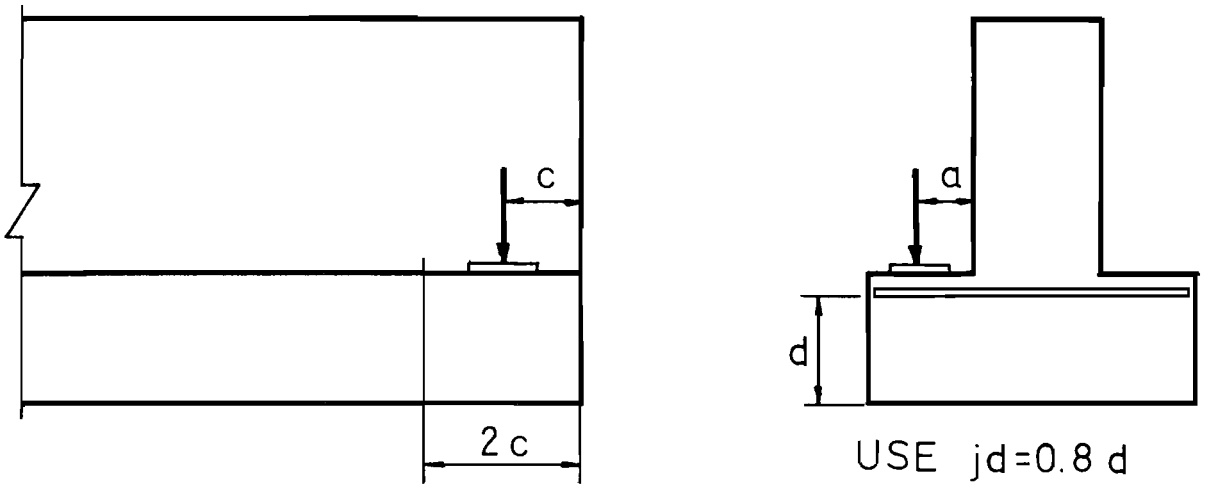

EFFECTIVE FOR FLEXURE

(b) NEAR END OF BEAM (c LESS THAN 2.5 a)

FIG. 38 - EFFECTIVE WIDTH OF BRACKET FOR FLEXURE.

effective width for flexure should contain all flexural steel required for the concentrated load, and compressive strength in concrete need not be checked.

(2) For flexural calculations of bracket reinforcement, the effective distance between the centroid of compression and the centroid of tensile force should be taken as jd = 0.8d.

(3) The depth of brackets d required to fulfill shear friction requirements should be taken as no less than

$$d_{min} = 1.5V_u/af'_c \qquad (4)$$

V_u = ultimate load applied to the bearing plate.
f'_c = the compressive strength of standard concrete cylinders.

Equation 4 is determined on the basis of the shear friction capacity of the concrete in the bracket acting over an effective width of 4a plus the width of bearing. Recommendations of the ACI 1971 Building Code would require that an area of steel reinforcement A_{vf} must extend into the bracket within the effective width according to the following formula:

$$A_{vf} = V_u/1.4\varphi f_y \qquad (3)$$

φ = a capacity reduction factor taken as 0.85.
f_y = the yield strength of reinforcement into the bracket.

(4) For values of a/d less than 0.5, shear friction requirements would govern the amount of steel through the web of the inverted T-beam into the top of the bracket, if one-third of the area A_{vf} were placed below the level of flexural steel. For a/d ratios higher than 0.5, flexural steel requirements would govern the amount of steel at the top of the bracket.

The behavior of the stem of the T-beam was studied by means of tests on one-third scale specimens. Observations of bracket behavior in full-scale specimens indicated the need for stirrups to act as hangers in

transmitting bracket loads up into the stem of the T-beam. In the presence of such stirrups acting as hangers there were observed no unique shear problems for inverted T-beams. The following conclusions were derived from observations of the model beam specimens:

(1) The ultimate shear strength of plain concrete (determined in accordance with minimum values in the ACI-71 Building Code) can be considered to act on all concrete between the compression face of the beam and the centroid of tensile steel. The area of concrete ordinarily considered as effective in preventing wide cracking due to shear includes only that concrete within the stem width b'.

(2) Stirrups should be designed to resist all ultimate shears above those resisted by concrete. For purposes of design it is not necessary to superimpose loads on stirrups acting as hangers and loads on stirrups acting as shear reinforcement.

(3) At every concentrated load applied to the bracket of an inverted T-beam, stirrups must be provided to act as hangers within a web depth d centered about the concentrated load. The capacity of hangers must be greater than the applied ultimate load.

(4) In summary, web reinforcement in the stem of an inverted T-beam must be proportioned on the basis of hanger requirements or shear strength requirements, whichever is larger. The two types of load on stirrups need not be superimposed for the design of web reinforcement.

All of the tests reported here involved the application of loads simultaneously to opposite sides of T-beam stems. In bridge structures the occurrence of maximum loading on both sides of bent cap girders is somewhat remote. There is a high probability that significant torsional forces on the inverted T-beam will be generated as traffic passes across the bent cap girder. The direction of torsional force reverses as traffic passes from one side across the girder to the other side. The consequences

of such torsion and torsion reversal will be studied in detail as a part of a subsequent project at the Center for Highway Research, The University of Texas at Austin.

REFERENCES

1. Timoshenko, S., and Woinowsky-Krieger, S., Theory of Plates and Shells, 2nd Edition, McGraw-Hill Book Co., New York, 1959, pp. 327-328.

2. "Building Code Requirements for Reinforced Concrete, Proposed Revisions of ACI 318-63," ACI Journal Proceedings V. 67, No. 2, February 1970, p. 115.

3. Timoshenko, S., and Goodier, J. N., Theory of Elasticity, 2nd Edition, McGraw-Hill Book Co., New York, 1951, pp. 99-106.

4. Howland, R. C. J., "Stress Systems in an Infinite Strip," Royal Society of Physics, Proceedings V, 124, 1929, Longon, p. 89.

5. Leonhardt, F., Walther, R., Dilger, W., "Shubversuche an indirekt gelagerten, einfeldrigen und durchlaufenden Stahlbetonbalken," Heft 201 des Deutscher Ausschuss Fur Stahlbeton, 1968.

6. Bauman, T., Rüsch, H., "Schubrersuche Fum Studium der Verdubelungswirkungder Biegezugbewchrung eines Stahlbetonbalken, Heft 201 des Deutscher Ausschuss Fur Stahlbeton, 1970.

7. Ferguson, P. E., "Some Simplifications of Recent Diagonal Tension Tests," ACI Journal Proceedings V. 53, No. 2, August 1956, pp. 157-172.